Hydrological soil properties control tree regrowth after forest disturbance in the forest-steppe of central Mongolia

Florian Schneider[1], Michael Klinge[1], Jannik Brodthuhn[1], Tino Peplau[2], Daniela Sauer[1]

[1]Department of Physical Geography, University of Göttingen, Göttingen, 37077, Germany
[2]Thünen Institute of Climate-Smart Agriculture, Braunschweig, 38116, Germany

Correspondence to: Florian Schneider (florian.schneider@uni-goettingen.de)

Abstract. The central Mongolian forest-steppe forms a transition between different ecozones and is as such particularly sensitive to environmental changes. It is commonly affected by disturbances such as logging and forest fires. Intensified drought events aggravate stress on the trees that are anyway at their drier limit in the forest-steppe. Climate change increases evapotranspiration and reduces the distribution of discontinuous permafrost, which leads to drier soil conditions. The motivation for this study came about through our previous observation that forest stands show great differences with respect to their recovery after disturbance by fire or logging. Sometimes, no regrowth of trees takes place at all. As water availability is the main limiting factor of forest growth in this region, we hypothesized that differences in soil hydrology control the forest-recovery pattern.

To test this hypothesis, we analysed soil properties under forests, predominantly consisting of Siberian larch (*Larix sibirica* Ledeb.), in the forest-steppe of the northern Khangai Mountains, central Mongolia. We distinguished four vegetation categories: 1. near-natural <u>for</u>est (FOR), 2. <u>ste</u>ppe close to the forest (STE), 3. <u>d</u>isturbed forest <u>wi</u>th <u>r</u>egrowth of trees (DWIR), and 4. <u>d</u>isturbed forest showing <u>no</u> <u>r</u>egrowth of trees (DNOR). 54 soil profiles were described in the field and sampled for soil chemical, physical, and hydrological analysis. We found a significant difference in soil texture between soils under DWIR and DNOR. Sand generally dominated the soil texture, but soils under DWIR had more silt and clay compared to soils under DNOR. Soil pF curves showed that soils under DWIR had higher plant-available field capacity in their uppermost parts than soils under DNOR. In addition, hydraulic conductivity tended to be higher in the uppermost horizons of soils under DWIR compared to their counterparts under DNOR. Chemical properties of the soils under DWIR and DNOR showed no significant differences.

We conclude that the differences in post-disturbance tree regrowth are mainly caused by different soil hydrology. High plant-available field capacity is the key factor for forest recovery under semi-arid conditions. High hydraulic conductivity in the uppermost soil horizons can further support tree regrowth, because it reduces evaporation loss and competition of larch saplings with grasses and herbs for water. Another important factor is human impact, particularly grazing on cleared forest sites, which often keeps seedlings from growing and thus inhibits forest recovery. None of the disturbed sites (DWIR, DNOR) had permafrost. We thus conclude that permafrost is no major factor for post-disturbance tree-regrowth pattern, although it

generally supports tree growth in the forest-steppe by preventing meltwater from seasonal ice from seeping below the root zone, thus increasing water supply in summer.

35 **Keywords:** Siberian larch, forest fire, human impact, climate change, soil hydrology, permafrost

1 Introduction

The forest-steppe in central Mongolia represents the transition between the Siberian taiga in the north and the Gobi Desert in the south, responding sensitively to climatic, ecological and anthropogenic disturbances. Water availability is the key factor that determines, where forest patches can exist within this landscape. Climate change is a major threat for the forest-steppe

40 due to aggravated drought stress (Allen et al., 2010). In Mongolia, intensified summer droughts became more frequent over the last century (Batima et al., 2005; Dashkhuu et al., 2015). Siberian larch (*Larix sibirica Ledeb.*), which is the dominant tree species in the Mongolian forest-steppe, suffers from these intensified droughts (Dulamsuren et al., 2010; Chenlemuge et al., 2015). Furthermore, summer droughts increase the risk of fires that disturb the vegetation structure in forests and reduce the size of the forest patches (Kharuk et al., 2008). This causes a negative effect on the forest microclimate, which in turn intensifies

45 the sensitivity of the forest to drought stress (Khansaritoreh et al., 2017a). In addition to fire, also human impact affects the structure of the forest stands. Logging and forest pasture reduce the forest size, open the forest stand and hamper post-disturbance forest regrowth (Khishigjargal et al., 2013; Tsogtbaatar, 2013; Dulamsuren et al., 2014).

Meltwater from the active layer above permafrost patches increases the soil-water availability and can thus support the survival of trees during drought events in summer (Sugimoto et al., 2002; Ishikawa et al., 2005; Churakova et al., 2016). Permafrost in

50 Mongolia is discontinuous and especially occurs under large forests. However, climate change is currently reducing the area of permafrost in Mongolia (Sharkhuu and Sharkhuu, 2012). After forest disturbance by fire or logging, permafrost degrades and may only reconstitute under certain conditions (Klinge et al., 2021). The loss of this additional water source leads to enhanced stress of trees during droughts.

Decreased water supply and increased drought stress raise the importance of soil properties in the Mongolian forest-steppe

55 even further. Soil-water distribution in the landscape after a rainfall event is generally controlled by bedrock, sediment cover, slope morphology and vegetation. In addition, plant-available field capacity and hydraulic conductivity of the soils influence the amount of water available at a site. Moreover, water repellency can reduce water infiltration, especially after fire events (DeBano, 2000; Doerr et al., 2000). Several studies have been conducted on soil distribution and soil properties in the Mongolian forest-steppe (Opp and Hilbig, 2003; Maximovich, 2004; Lehmkuhl et al., 2011). Nandintsetseg and Shinoda

60 (2011) modelled soil moisture conditions in Mongolia based on data from meteorological stations from 1986 until 2005. They obtained a gradient of increasing soil moisture from southwest to northeast during summer. Haase (1963) studied soils in relation to altitudinal zones in the Khangai Mountains, including particle size distribution, chemical soil properties, and water content. He reported forest vegetation on soils with higher water content and predominant steppe vegetation on soils with lower water content. However, he focused mainly on general soil description and did not report any further details on soil-

2

65   vegetation relationships. Krasnoshchekov (2008, 2010) described physical and chemical soil properties in the East Khubsugul region and the Khangai Mountains. Sympilova and Gyninova (2012) conducted similar research in the Selenga Mountains. However, in both studies only the soils were characterised, without linking them to the vegetation pattern. Sommer (2000) analysed soils of the forest-steppe of the Turgen-Charchiraa-Mountains in north-western Mongolia. He focused on soil-chemical aspects and did not find a clear relationship between forest distribution and soil properties. He concluded that forest

70   distribution was climate-controlled and disturbed by pastoral pressure and logging. Yet, he did not analyse soil-hydrological properties.

    During previous fieldwork in the Khangai Mountains, in the central Mongolian forest-steppe, we observed that forest regrowth after disturbance does not proceed equally. The post-disturbance development of forest stands with apparently same site conditions ranges from spontaneous dense regrowth to no regrowth at all. As the trees are at their drier limit in this sensitive

75   landscape, we assumed that water availability is the main factor that controls forest regrowth after disturbance, whereas nutrient availability plays a less important role. Since both factors are related to soil properties, we established the following hypotheses:

1) Silty soil texture leads to high plant-available field capacity and is thus favourable for post-disturbance tree regrowth.

2) High hydraulic conductivity in the uppermost parts of the soils supports post-disturbance forest regrowth, as rapid water
80   infiltration to some depth reduces evaporation and ground-vegetation transpiration.

3) High nutrient stocks, for example after fire events, may support post-disturbance forest regrowth, unless nutrient stocks are anyway well above the requirements of Siberian larch. In this case, no effect is to be expected.

4) Permafrost may increase water availability for trees through the continuous water release at the melting front above the permafrost table over the summer season. As water above the permafrost table cannot infiltrate downwards, interflow may
85   occur above the permafrost table. This process leads to increased water availability, especially in concave slope positions where interflow converges. Thus, permafrost may support post-disturbance forest regrowth also at sites with otherwise unfavourable soil-hydrological conditions for forest regrowth.
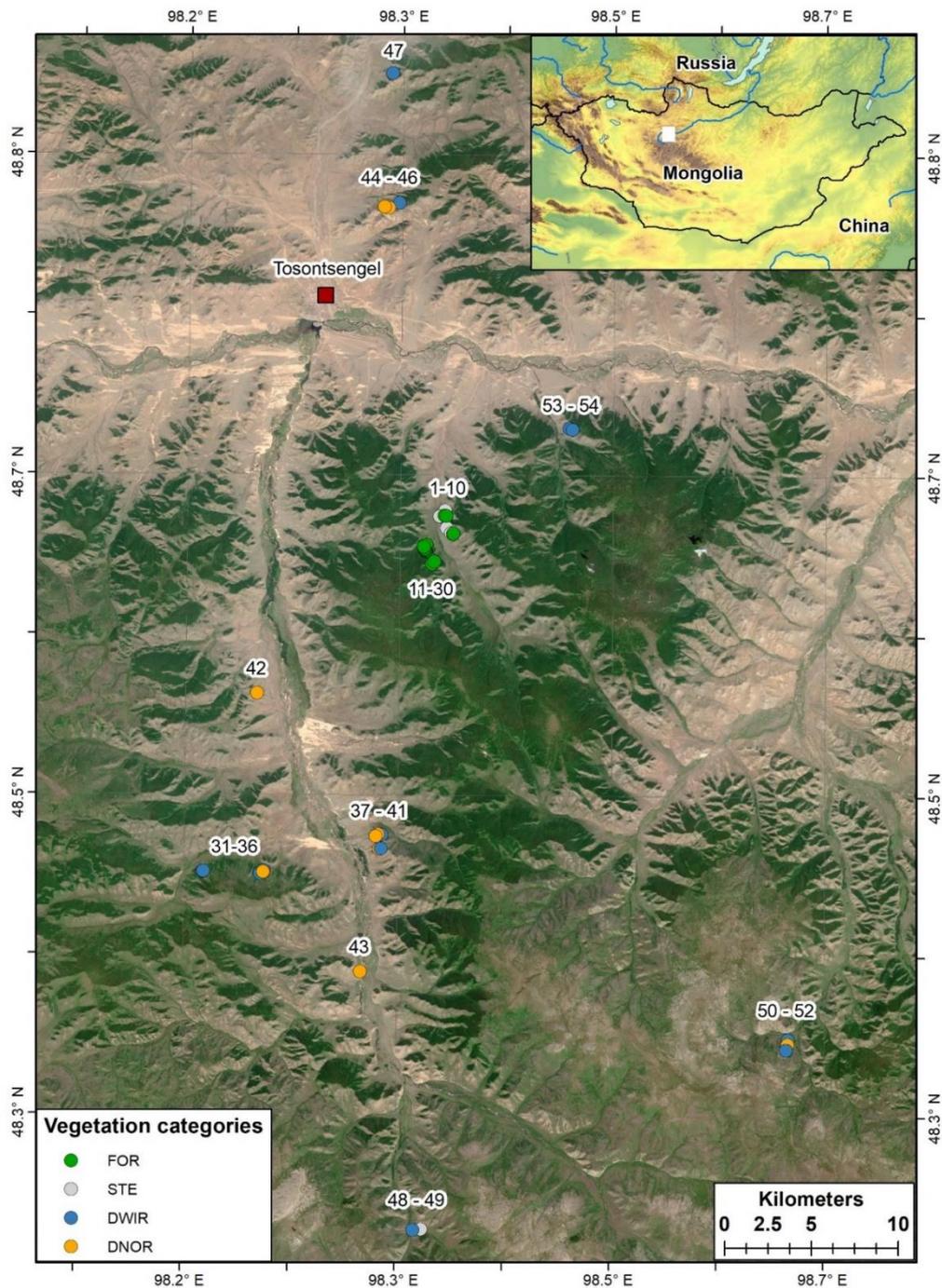
2 Materials and methods

2.1 Study area

90   The study area was located in the central Mongolian forest-steppe, in the northern Khangai Mountains, near the town Tosontsengel (Fig. 1). The geological basement predominantly consists of Permian acidic plutonic and metamorphic sedimentary rock, with some occurrences of Carboniferous mafic rock (Academy of Sciences of Mongolia, Academy of Sciences of USSR, 1990). Slope debris with inmixed aeolian sand and silt provides the parent material for the soils in the region. The widespread aeolian deposits originate from lacustrine sediments of big lakes that dried out during the glacial

95 periods in the Basin of Great Lakes, located between the Mongolian Altai and the Khangai Mountains (Grunert et al., 2000; Lehmkuhl and Haselein, 2000; Klinge and Lehmkuhl, 2013).

The climate is cold, semi-arid, and highly continental. In the town Tosontsengel, in the northern part of the study area, mean monthly temperatures range from -31.7 °C in January to 14.9 °C in July (see supplement Figure_S1). Mean annual precipitation is 200-500 mm. Rainfall concentrates in summer, because of low-pressure cells that are blown in with the westerlies (Batima 100 et al., 2005). The mean annual temperature of -5.9 °C supports discontinuous permafrost in the study area (Bonan and Shugart, 1989). Permafrost patches occur on forested slopes, where the canopy protects them from solar radiation, and the organic layer insulates them from high air temperatures in summer (Dashtseren et al., 2014). In summer, the forests benefit from an additional water supply by meltwater from the active layer above the permafrost (Zhang et al., 2011).

Figure 1: Sentinel image (2019/07/31) of the study area with soil profile positions. The colours indicate the four vegetation categories that were used for selecting the soil profile locations: near-natural forest (FOR, green), steppe close to forest (STE, grey), disturbed forest with regrowth of trees (DWIR, blue), and disturbed forest showing no regrowth of trees (DNOR, orange). The soil profiles are listed in Table 1 of the appendix. Right top: Physical map of Mongolia, showing the location of the study area (white rectangle).

The vegetation of the study area is dominated by steppe. Only north-facing slopes and some valley positions are covered by

110 forest, predominately consisting of Siberian larch (Hilbig, 1987; Tsogtbaatar, 2013). The understory of these forests varies with respect to proportions of grasses, herbs, mosses and shrubs (commonly including e.g. *Vaccinium vitis-idea* and *Lonicera altaica*). High evapotranspiration combined with low precipitation and relief-dependant differences in insolation control the vegetation pattern (Schlütz et al., 2008; Hais et al., 2016). The semi-arid conditions promote frequent forest fires in this region (Goldammer, 2002; Hessl et al., 2016). The last two severe fire events in the study area happened in 1996 and 2002.

115 A timber factory was established in the 1960s in Tosontsengel. Thus, logging strongly affected the forest stands in the study area. Since the 1990s, industrial logging is abandoned, but illegal logging is still common (Lkhagvadorj et al., 2013). Moreover, pastoral pressure increased over the last decades (Lkhagvadorj et al., 2013). Logging, followed by grazing, led to a reduction of the forested area, especially at its lower boundary and at the forest edges.

2.2 Field work

120 The site selection within the study area was based on four categories of vegetation: near-natural <u>for</u>est (FOR), <u>ste</u>ppe close to forest (STE), <u>d</u>isturbed forest <u>wi</u>th regrowth of trees (DWIR) and <u>d</u>isturbed forest showing <u>no</u> regrowth of trees (DNOR) (Figs. 1 and 2). In addition, we distinguished three categories of disturbance intensity. "Low intensity" included e.g. logging of single trees. "Moderate" included logging of patches within a forest stand and fires that did not affect the whole forest stand. "Severe" included clear cutting and fires that destroyed the whole forest stand (Tab. A1, appendix). To reduce the effects of factors that

125 were not in the focus of this study, we kept geology, exposition (only north-facing slopes), inclination, and slope morphology as similar as possible. Elevation of the studied soil profiles ranged from 1850 to 2100 m a.s.l., which is well below the upper tree line of approx. 2500 m a.s.l. (Klinge et al., 2018). 54 soil profiles were described according to the FAO Guidelines for Soil Description (Jahn et al., 2006) and classified according to WRB (IUSS Working Group WRB, 2015). The presence of permafrost was documented as well. The soil profiles were sampled horizon-wise, whereby thick horizons were subdivided

130 for the sampling, such that the maximum thickness included in one sample did not exceed 30 centimetres. We also carried out *in situ* measurements of saturated hydraulic conductivity, using a compact constant-head permeameter (Eijkelkamp) (Amoozegar and Warrick, 1986; USDA, 2014). The measurements were done in five replicates. In addition, soil horizons with low rock-fragment contents were sampled with 100 cm³ and 250 cm³ steel cylinders for laboratory measurements of pF curves and hydraulic conductivity, respectively. Samples for pF curves were taken during two field campaigns, whereas samples for

135 hydraulic conductivity were taken only during one field campaign, thus not from all profiles that were sampled for pF measurements. The in-situ measurements of hydraulic conductivity provided additional data. Therefore, the sizes of the datasets for pF curves and hydraulic conductivity differ.
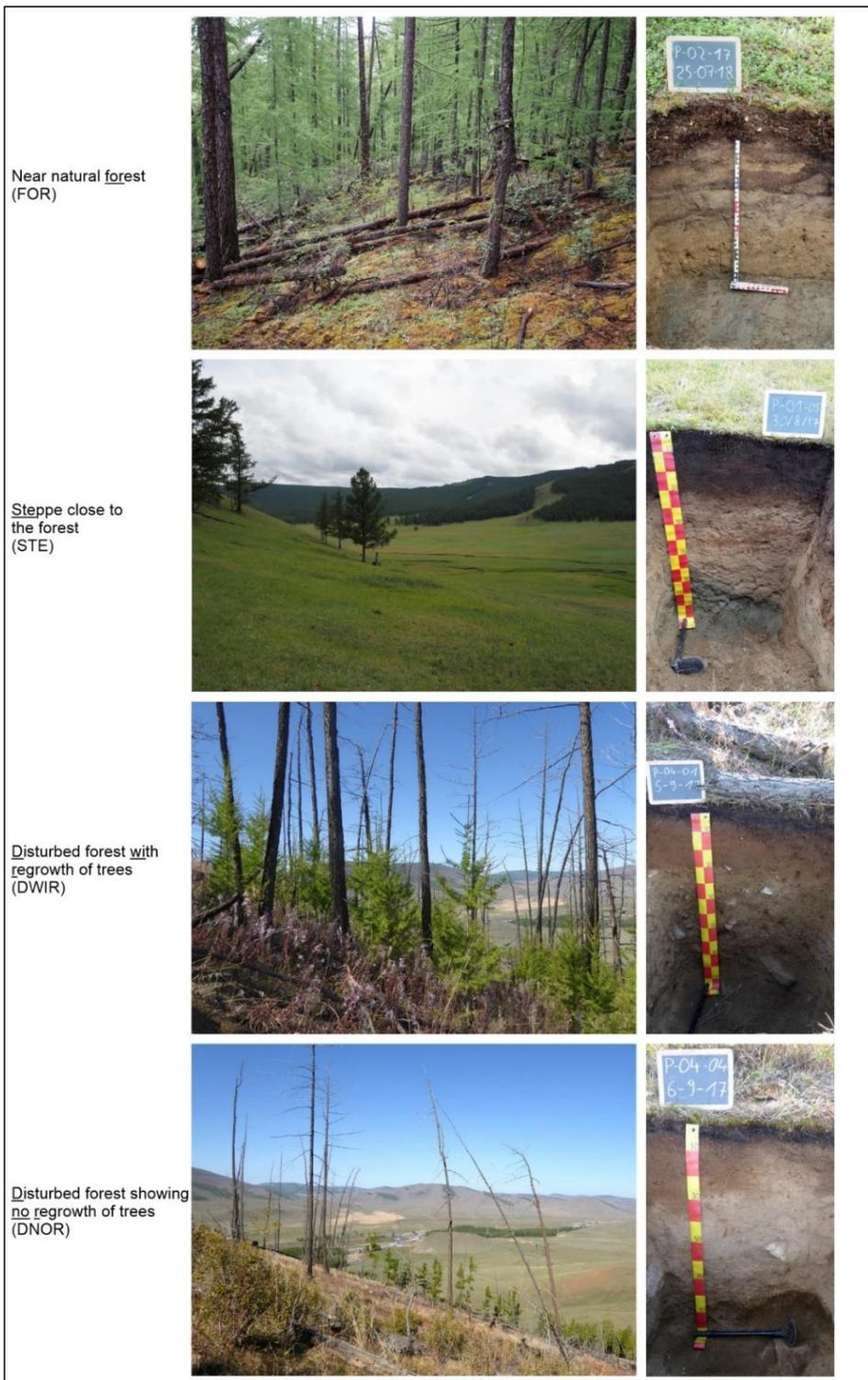
Figure 2: Typical soil profiles under the four vegetation categories.

2.3 Laboratory analyses

The soil samples were dried at 40 °C and passed through a 2 mm sieve. Approximately 10 g of each sample was dried at 105 °C to gravimetrically determine the remaining water contents for correcting all analytical data obtained from the 40 °C-dried samples. An aliquot of each sample was milled. Total C and N contents were analysed on the milled samples using a CHN analyser (LecoTruSpec). Carbonate contents were also analysed on the milled samples using the Scheibler method. Soil organic carbon (SOC) contents were calculated by subtracting soil inorganic C (obtained from carbonate analysis) from total C. Soil pH was measured in 1M KCl solution at a soil:solution ratio of 1:5. Exchangeable Al, Fe, Mn, Ca, Mg, K, and Na were extracted with 1 M ammonium chloride solution and measured by use of an ICP-OES (Thermo Scientific). The effective cation exchange capacity (ECEC) was calculated as the sum of negative charges occupied by these exchangeable cations. Pre-treatments for particle size distribution analysis were as follows: Soil organic matter was removed by 30 % H_2O_2, carbonates were dissolved, if necessary, by 10 % hydrochloric acid, and micro-aggregates were dispersed by 0.4 M sodium pyrophosphate. The three sand fractions were separated by sieving, and the silt and clay fractions were determined by use of a sedigraph (micromeritics). Bulk density was estimated in the field (Jahn et al., 2006) and measured on undisturbed samples in the laboratory. All element concentrations in the fine earth were converted to element stocks per m² considering rock-fragment content and bulk density.

Hydraulic conductivity and pF curves were determined on 41 of the soil profiles under FOR, DWIR and DNOR. Hydraulic conductivity was measured in five replicates, using a permeability device with falling water head (self-constructed device based on German norm DIN 19683-9). Soil pF curves were determined in four to five replicates, using a pressure device (ecoTech). The cylinders with the samples were carefully water saturated and placed on ceramic plates in the pressure pots. Pressures corresponding to pF 1.8, 2.5 and 4.2 were applied and the weight of the samples at each pF was determined. Water repellency was analysed on five replicates for each top-soil sample (Doerr, 1998). The sample was placed in a petri dish and the surface was manually smoothened. The time was measured until a drop of distilled water, released from a pipette at 5 cm above the sample surface, infiltrated into the sample.

2.4 Data processing and statistical analysis

We described and sampled the soil profiles down to either the bedrock or permafrost, resulting in a maximum depth of 180 cm. According to the literature, the roots of Siberian larch can reach this depth (Kapper, 1954; Albenskiy et al., 1956). Therefore, we included all soil horizons in the calculations of element stocks to evaluate the nutrient availability for larch trees at a site. To assess in addition the site conditions also for tree seedlings without fully developed root system, we only used the properties of the uppermost 10 cm of the soils. For this purpose, we calculated the weighted means of the following variables for the uppermost 10 cm of the soils: content of rock fragments, bulk density, H+ concentration (log (10^{-pH})), carbonate content, clay content, silt content, sand content, and ECEC (first group of variables). Element contents in the fine earth of each horizon were converted to element stocks per horizon (considering rock fragment content and bulk density), and were summed up over

8

the uppermost 10 cm of the soils. This was done for exchangeable Al, Ca, K, Na, Mg, Mn, Fe, SOC, and total N (TN) (second group of variables).

All statistical analyses were carried out with the R project for statistical computing (R Core Team, 2014). The share of each horizon in the uppermost 10 cm of the soil was used for the weighting, based on formula $x1$ (1) for the first group of variables, and formula $x2$ (2) for the second group of variables.

$x1 = if\ (upper\ boundary > 10)\ \{NA\}\ else\ \{$
$\quad\quad if\ (lower\ boundary <= 10)\ \{(lower\ boundary - upper\ boundary)/10\}$
$\quad\quad else\ \{(10 - upper\ boundary)/10\}\},$ (1)

$x2 = if\ (upper\ boundary > 10)\ \{NA\}\ else\ \{$
$\quad\quad if\ (lower\ boundary <= 10)\ \{1\}$
$\quad\quad else\ \{((lower\ boundary - upper\ boundary) - (lower\ boundary - 10))/(lower\ boundary -$
$upper\ boundary)\}\}$ (2)

We conducted all statistical analyses (i) on the entire data set of each profile, and (ii) on only the data of the uppermost 10 cm of each profile. All analyses and graphical representations were performed with the R packages "aqp", "ggplot2" and "ggpubr" (Beaudette et al., 2013; Wickham, 2016; Kassambara, 2019). Principle component analyses (PCAs) were calculated and graphically depicted with the R packages "FactoMineR" and "factoextra" (Lê et al., 2008; Kassambara and Mundt, 2019). The PCAs were used to identify relations between the variables and the samples. The PCA of the uppermost 10 cm of the soils also included inclination, exposition and elevation. Linear regression models were used to compare the data obtained for soils under DWIR and DNOR. The results, including 95 % confidence intervals, described the differences between the soils under DWIR and DNOR.

We did not subject measured plant-available field capacity (FC$_{pa}$) and hydraulic conductivity to statistical analysis because of their unequal representation of the vegetation groups. Although we tried to sample as many profiles as possible, high rock-fragment contents prevented equal sampling of soils under the different vegetation groups and resulted in a small number of samples. Thus, we only present the measured data in a site-wise comparison to prevent any bias.

In addition, we applied a pedo-transfer function to estimate FC$_{pa}$ for all soil horizons, based on other measured soil parameters that were available for all samples. We tested several transfer functions from literature and chose the function established by Gupta and Larson (1979) because it matched best with our measured pF data, is based on a large dataset (43 soils and a test run on 61 soils), and, included a wide range of different soils (0-65 % clay content, 1-72 % silt content, 5-98 % sand content, 0.74-1.74 g*cm^{-3} bulk density) (see supplement Table_S1). We calculated the plant-available field capacity (FC$_{pa,cal}$) as follows:

9

$$FC_{pa,cal}(vol.\%) = ((0.005678 * sand(\%) + 0.009228 * silt(\%) + 0.009135 * clay(\%) + 0.006103 * C_{org}(\%) - 0.2696 * bulk\ density(g * cm^{-3})\ ) - (-0.000059 * sand(\%) + 0.001142 * silt(\%) + 0.005766 * clay(\%) + 0.002228 * C_{org}(\%) + 0.02671 * bulk\ density(g * cm^{-3})) * 100 \tag{3}$$

The results were multiplied by fine-earth content [vol.%], thus assuming that rock-fragments did not contribute to FC_{pa}. We deleted three values from the resulting $FC_{pa,cal}$ dataset because they exceeded a $FC_{pa,cal}$ of 40 vol.%, which we considered unrealistic.

3 Results

3.1 Field observations

The bedrock in the study area predominantly consisted of granite, with some minor occurrences of gneiss. Thick aeolian sand sheets locally covered the lower slopes and valley bottoms along west-east running valleys (Fig. 1). Thus, carbonates that were observed in some of the soils were supposed to originate from aeolian deposits.

The parent materials of the soils on the slopes generally consisted of a vertical succession of two to three sediment layers. The lowermost one was typically a solifluction layer, characterised by a high content of rock fragments with sizes ranging from fine gravel to angular stones. This layer was usually overlain by another slope deposit, consisting of a mixture of weathering products of the bedrock, and aeolian sand and silt. This slope deposit showed lower rock-fragment contents than the underlying one, but similar rock-fragment sizes. The proportions of sand and silt in the upper slope deposit varied both within a profile and between the profiles. In places, a Holocene colluvial deposit with varying thickness covered the slope deposits described above. Our profiles 4, 5 and 38 predominantly consisted of Holocene colluvium, whereas most of the other profiles included either no or only a thin Holocene colluvial deposit. The Holocene colluvial deposits had very low contents of rock fragments that typically consisted of fine to medium gravel. At three sites, only a thin sediment layer covered the bedrock (profiles 3, 47, 52). As an exception, the parent material at one of the forest sites (profiles 1, 2, 7, 8, 9) consisted of a slope deposit with extremely high proportions of aeolian sand.

Phaeozems and Cambisols were the most common soils under the near-natural forests (FOR) and disturbed areas (DWIR, DNOR). In addition, Cryosols occurred above permafrost patches. Soils under steppe (STE) included Phaeozems, Chernozems, and Kastanozems. The soil structure of the A horizons was generally granular, the B horizons had subangular or angular blocky structure, and the C horizons had single grain, massive or rock structure. Rock fragments in several C horizons showed manganese or carbonate pendants (Tab. A1, appendix). Bioturbation by rodents was observed in the soils at one forest site (profiles 1, 2, 7, 8, 9), whereas cryoturbation was not found at any of the investigated sites, most likely because of insufficient moisture. Charcoal was present in most of the topsoils.

Human impact affected most of the sites, except for the near-natural forest sites (FOR) that showed either no or only minor disturbance such as cutting of single trees. Disturbance in DWIR and DNOR varied between moderate and severe. Most of the
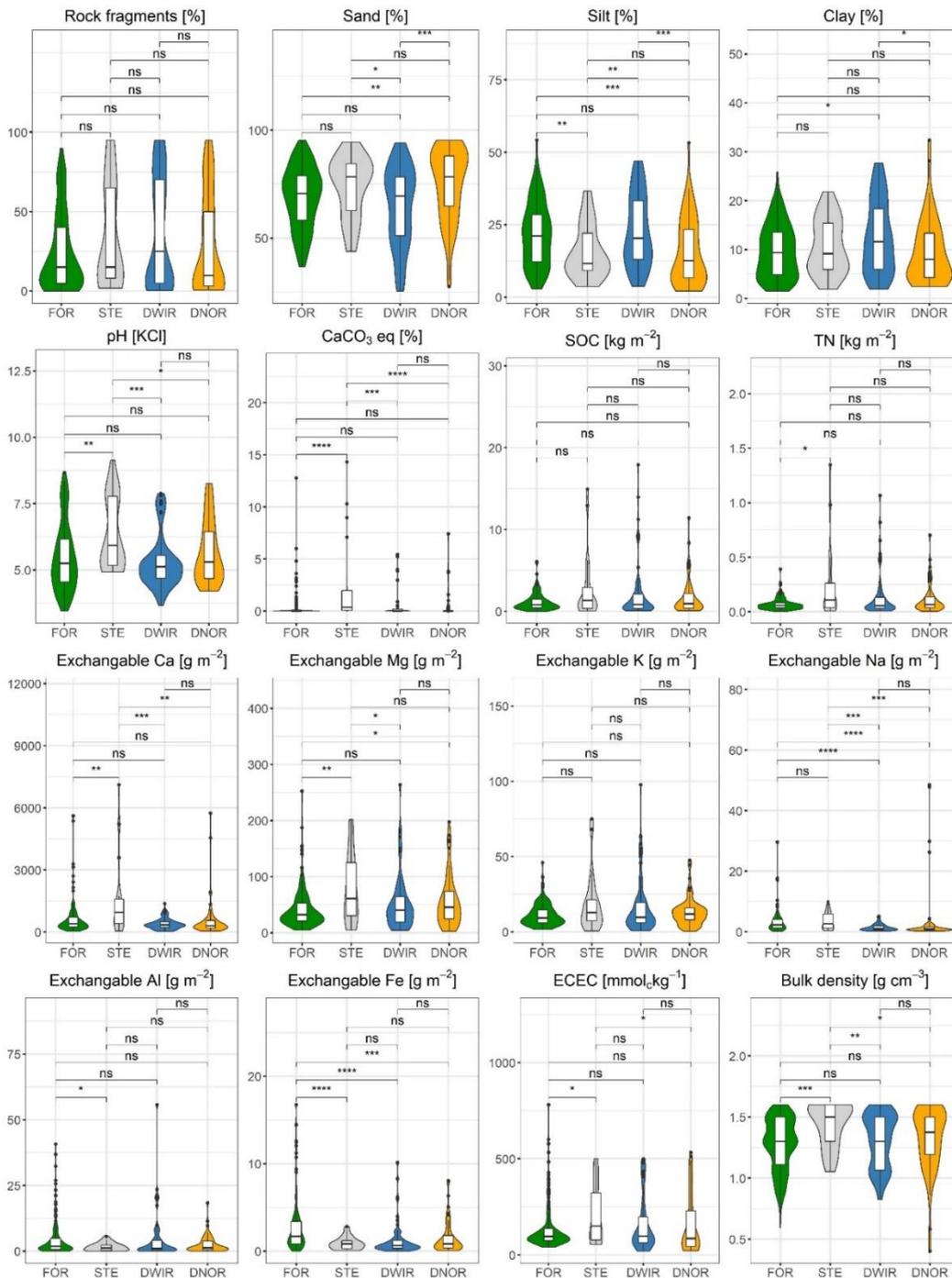
sites were impacted by both fire and logging; yet, some profiles were only affected by one type of disturbance (Tab. A1, appendix).

Permafrost was only encountered in soil profiles under near-natural <u>for</u>est (FOR). The depth of the permafrost table varied between 60 cm and 100 cm in soils on slope debris under closed forests, and between 140 cm and 180 cm in soils on sandy deposits under open forests (Tab. A1, appendix). In soils under STE, DWIR, and DNOR no permafrost was present above the bedrock that was typically encountered between 80 cm and 110 cm soil depth.
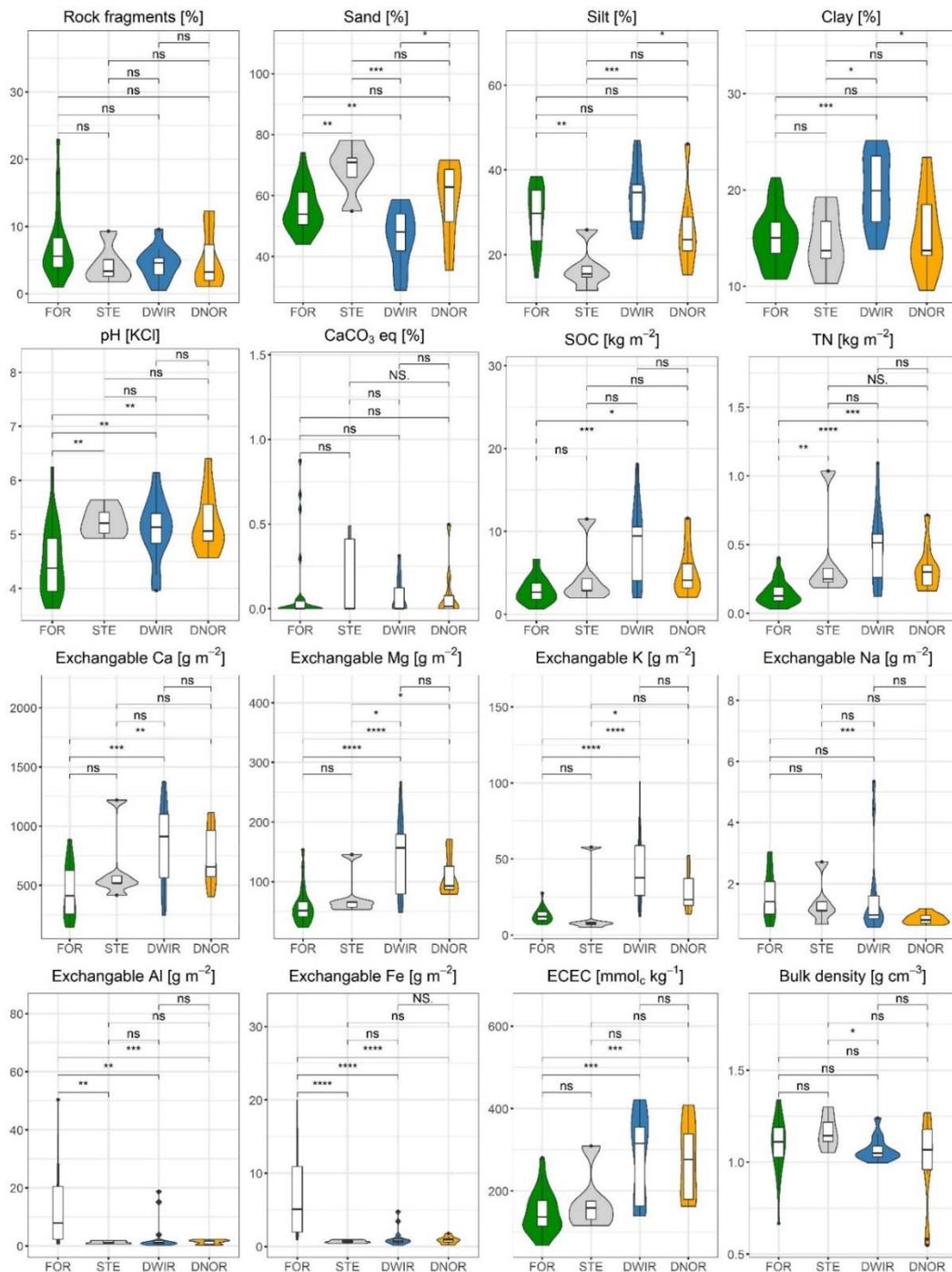
3.2 Chemical and physical soil properties

Comparison of the entire soil profiles (down to either the bedrock or permafrost) showed that soils under STE had significantly higher contents of carbonates and exchangeable Ca than soils under all other vegetation categories (Fig. 3), whereas soils under FOR had significantly higher contents of exchangeable Fe compared to soils under all other vegetation categories. There were no statistically significant differences between soils under DWIR and DNOR with respect to rock-fragment contents, SOC and TN stocks, pH, contents of exchangeable Mg, K, Na, Al, Mn, and ECEC. However, soils under DWIR and DNOR differed significantly in their particle size distribution: Soils under DWIR had higher silt and clay contents, whereas soils under DNOR had higher sand contents. Soils under FOR had similar silt contents as soils under DWIR, whereas soils under STE had similar sand contents as soils under DNOR. Bulk density of soils under FOR and DWIR was lower than that of soils under DNOR. Yet, there was only a significant difference in bulk density between soils under FOR and DNOR but not between soils under DWIR and DNOR.

Comparison of only the uppermost 10 cm of each soil profile (for evaluating the soil conditions for tree seedlings) suggested that soils under DWIR had larger stocks of exchangeable Mg and K, SOC and TN than soils under DNOR, however without significant differences (Fig. 4). The other chemical soil properties showed no differences between soils under DWIR and DNOR. In contrast, particle size distribution showed again a significant difference between soils under DWIR and DNOR. Soils under STE had the highest sand contents, followed by soils under DNOR. Soils under DWIR had the highest clay and silt contents, followed by soils under FOR. Bulk densities and rock-fragment contents of the soils of the four vegetation categories were similar.

Figure 3: Properties of the entire soil profiles (down to either the bedrock or permafrost) under the four vegetation categories (n = 305): near-natural forest (FOR, green), steppe close to the forest (STE, grey), disturbed forest with regrowth of trees (DWIR, blue) and disturbed forest showing no regrowth of trees (DNOR, orange). P values indicated above the plots were calculated for differences between the arithmetic means (ns: p > 0.05; *: p ≤ 0.05; **: p ≤ 0.01; ***: p ≤ 0.001; ****: p ≤ 0.0001). Horizontal bars = medians, boxes = first and third quartiles, points = outliers, violins = data distributions.

Figure 4: Properties of the uppermost 10 cm of the soil profiles under the four vegetation categories (n = 54): near-natural forest (FOR, green), steppe close to the forest (STE, grey), disturbed forest with regrowth of trees (DWIR, blue) and disturbed forest showing no regrowth of trees (DNOR, orange). P values indicated above the plots were calculated for differences between the arithmetic means (NS.: p = 1; ns: p > 0.05; *: p ≤ 0.05; **: p ≤ 0.01; ***: p ≤ 0.001; ****: p ≤ 0.0001). Horizontal bars = medians, boxes = first and third quartiles, points = outliers, violins = data distributions.
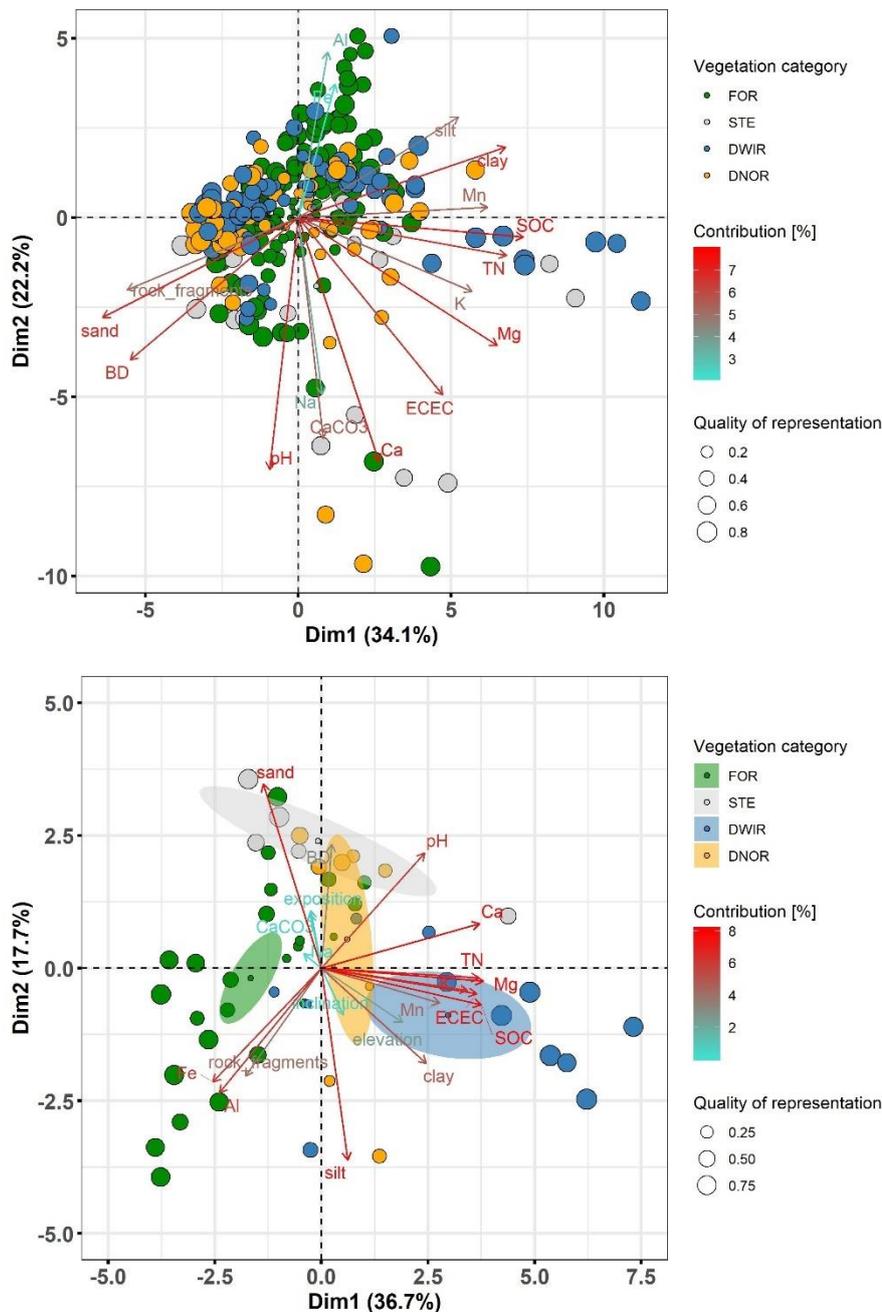
Figure 5: Top: PCA of the properties of the entire soil profiles under the four vegetation categories (n = 303): near-natural forest (FOR, green), steppe close to the forest (STE, grey), disturbed forest with regrowth of trees (DWIR, blue) and disturbed forest showing no regrowth of trees (DNOR, orange). **Bottom:** PCA of the properties of the uppermost 10 cm of the soil profiles under the four vegetation categories (n = 52). In addition, inclination, exposition and elevation were included in the second PCA. Arithmetic means and 95 % confidence intervals of the data for soils under each vegetation category are represented by a smaller circle and a shaded ellipse, respectively. SOC = soil organic carbon, TN = total nitrogen, ECEC = effective cation exchange capacity, BD = bulk density, and Ca, Mg, K, Na, Al, Fe, and Mn = exchangeable cations.

14

In the principle component analysis (PCA) of the data for the entire soil profiles, the first two factors explained 56.3 % of the
280   total variance (Fig. 5 top). The variables sand content, rock-fragment content and bulk density on one hand, made up one axis
together with clay and silt contents on the other hand. Most of the data scattered around this axis, regardless of vegetation
category. Exchangeable Al and Fe on one hand, made up a second axis together with pH, carbonate content, and exchangeable
Ca and Na on the other hand. Exchangeable Al and Fe did not contribute much to the PCA, yet, the soils under FOR clustered
around them. On the other hand, some soils under STE, DNOR and FOR clustered around pH, carbonate content, and
285   exchangeable Ca and Na. In addition, another cluster around SOC and TN stocks, and exchangeable Mg, K and Mn, occurred
close to the axis of clay and silt contents. Mainly soils under DWIR but also some soils under STE fell into this cluster.
In the PCA of the data for the uppermost 10 cm of the soil profiles, the first two factors explained 54.5 % of the total variance
(Fig. 5 bottom). Sand content and bulk density on one hand, made up one axis together with silt content on the other hand.
Rock-fragment content and exchangeable Fe and Al on one hand, made up a second axis together with pH on the other hand.
290   In addition, a cluster of clay content, SOC and TN stocks, ECEC, and exchangeable Mg, K and Mn occurred. The factor
elevation also fell into this cluster, but with a minor contribution. The contributions of inclination, exposition, carbonate
content, and exchangeable Na were negligible. In general, the data for the uppermost 10 cm of the soils under the four
vegetation categories (lower PCA) plotted more separately from each other than those for the entire soil profiles (upper PCA).
The arithmetic means and 95 % confidence intervals of the data for the uppermost 10 cm of the soils under the four vegetation
295   categories (smaller dots and shaded ellipses) confirmed the differences and clear separation. Soils under FOR plotted around
the axes of sand and exchangeable Fe and Al. Soils under STE concentrated around sand and bulk density, thereby slightly
shifting to the side of exchangeable Ca, Mg, K, and SOC and TN stocks. Soils under DWIR plotted closer to silt than to sand,
and mostly fell into the cluster of ECEC, exchangeable Mg, K, and SOC and TN stocks. Soils under DNOR plotted between
those under STE and DWIR. The confidence interval of the soils under FOR was clearly separated from all other confidence
300   intervals. That of the soils under DWIR was also separated and showed only a minor overlap with the one of soils under
DNOR. The confidence intervals of the soils under STE and DNOR showed a considerable overlap.

Based on the data presented in Figures 3-5, we chose the most relevant variables for direct comparison of the soil properties
under DWIR and DNOR, using multiple linear regression models (Fig. 6). We found a significant difference in particle size
305   distribution, both for the data of the entire soil profiles (Fig. 6 top) and for the uppermost 10 cm of the soil profiles (Fig 6.
bottom). Soils under DNOR had clearly more sand, and less silt and clay than soils under DWIR. The soils did not exhibit
significant differences with respect to any other soil properties. All confidence intervals overlapped with the zero line, and all
p values were >0.05. The only relevant observation was that the uppermost 10 cm of the soil profiles under DNOR tended to
have smaller stocks of SOC and exchangeable K, compared to those under DWIR, however without significant differences
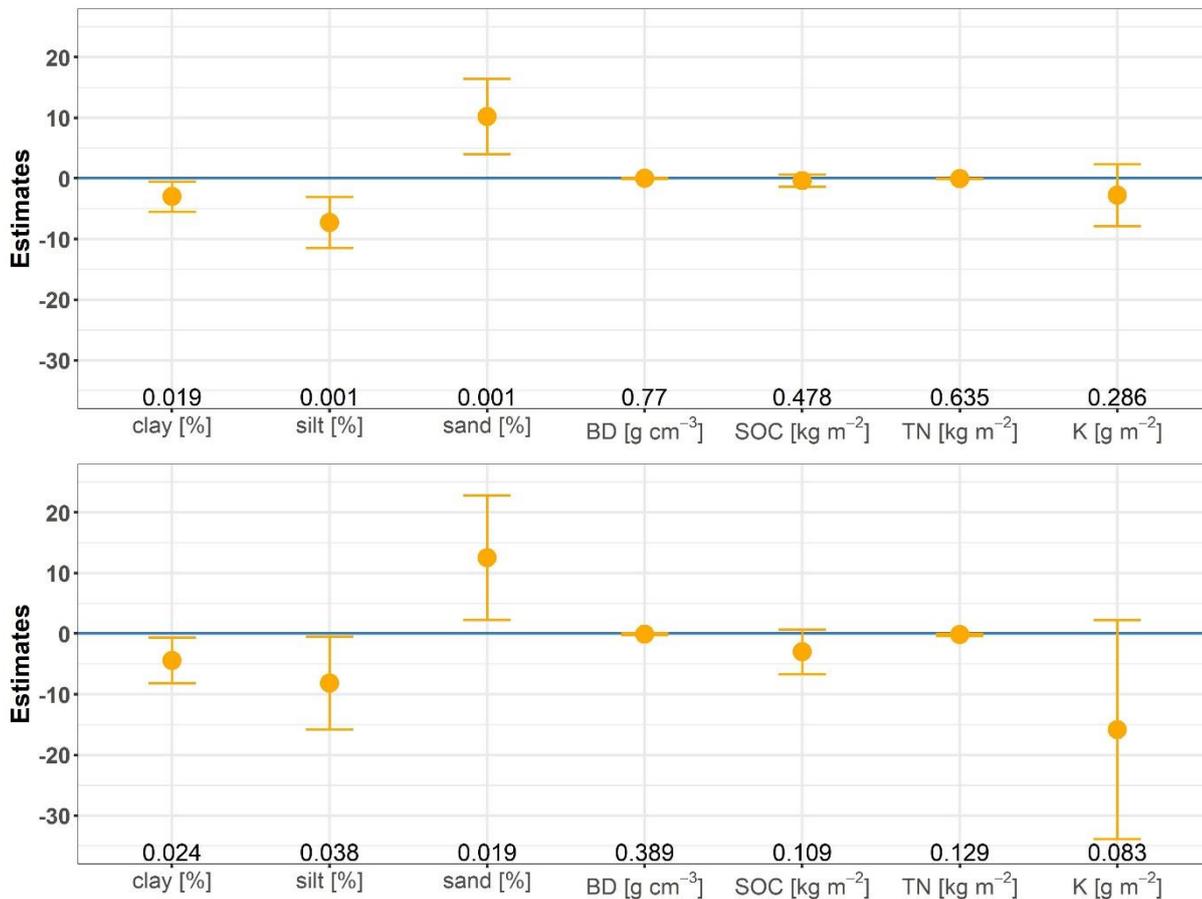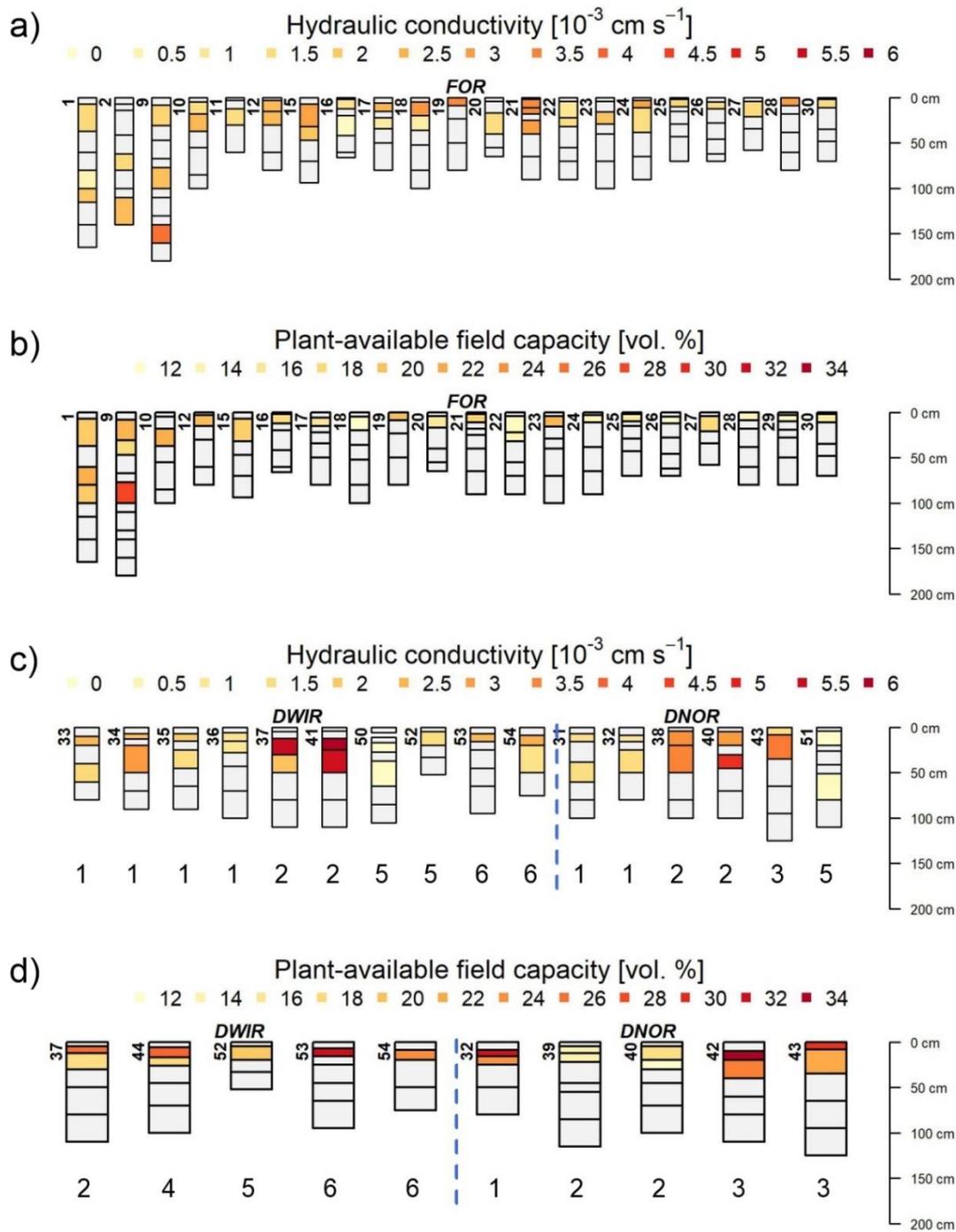310   either.

15

Figure 6: Top: Estimates and 95 % confidence intervals of linear regression models, comparing the entire soil profiles under disturbed forest showing no regrowth of trees (DNOR, orange) to those under disturbed forest with regrowth of trees (DWIR, blue) (n = 305). P values indicated below the plots were calculated for the differences between the estimates for soils under DNOR and DWIR. Data for exchangeable Mg were left out for better readability (estimate: +4.5; confidence intervals: +21.2/-12.2; p = 0.596). Bottom: Estimates and 95 % confidence intervals of linear regression models, comparing the uppermost 10 cm of the soil profiles under DNOR (orange) to those under DWIR (blue) (n = 54). P values indicated below the plots were calculated for the differences between the estimates for soils under DNOR and DWIR. Data for exchangeable Mg were left out for better readability (estimate: -32.2; confidence intervals: +16.5/-80.9; p = 0.184). BD = bulk density, SOC = soil organic carbon, TN = total nitrogen, K = exchangeable potassium.
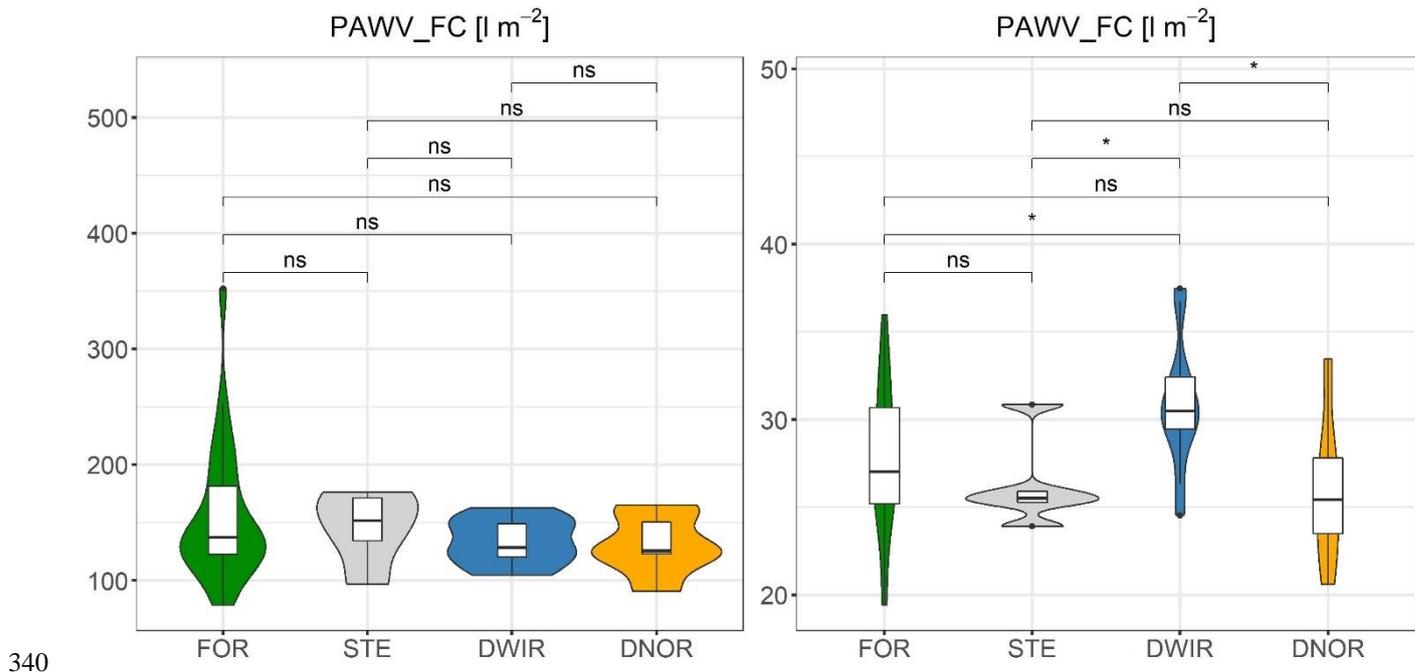
3.3 Hydrological soil properties

In general, all soils had high hydraulic conductivities, due to their predominantly sandy texture. A site-wise comparison between soils under DWIR and DNOR showed that soils under DWIR tended to have higher hydraulic conductivities in their uppermost horizons (Fig. 7 bottom). For example, the hydraulic conductivities of soil profiles 31 and 32 (DNOR) at site 1 were below $1.5 \cdot 10^{-3}$ cm s^{-1} whereas those of profiles 33 – 36 (DWIR) ranged between 1.5 and $3 \cdot 10^{-3}$ cm s^{-1}. Profiles 38 and 40 (DNOR) at site 2 showed hydraulic conductivities between $2.5 \cdot 10^{-3}$ cm s^{-1} and $3.5 \cdot 10^{-3}$ cm s^{-1} in their uppermost horizons, while the hydraulic conductivities of profiles 37 and 41 (DWIR) exceeded $5 \cdot 10^{-3}$ cm s^{-1}. Soils under FOR showed similar

16

hydraulic conductivities, with a maximum of 3.5 10^{-3} cm s^{-1} (Fig. 7 top). Soils under FOR had lower plant-available field capacities (FC_{pa}) than soils under DWIR and DNOR (Fig. 7). Except for one subsoil horizon, FC_{pa} ranged from 12 vol. % to 330   22 vol. % in soils under FOR, and from 12 vol. % to 33 vol. % in soils under DWIR and DNOR. The differences between soils under DWIR and DNOR became clearer in a site-wise comparison. For example, FC_{pa} of profiles 39 and 40 (DNOR) at site 2 ranged between 12 vol. % and 17 vol. %, whereas profile 37 (DWIR) had FC_{pa} between 17 vol. % and 26 vol. %. However, the limited number of samples analysed for FC_{pa} did not allow for a final statement on differences between the sites with respect to FC_{pa}.

17

Figure 7: Hydraulic conductivities (a) and plant-available field capacities (b) of soils under near-natural forest (FOR), and hydraulic conductivities (c) and plant-available field capacities (d) of soils under disturbed forest with regrowth of trees (DWIR; left) and under disturbed forest showing no regrowth of trees (DNOR; right). Soil horizons in light grey colour were not subjected to these measurements. Same numbers under the profiles in (c) and (d) indicate that the profiles were located at the same site.

18

Figure 8: Calculated plant-available water volume at field capacity (PAWV$_{FC}$) per square metre, stored in the entire soil profiles (left), and stored in only the uppermost 10 cm of the soil profiles (right) under the four vegetation categories: near-natural forest (FOR, green), steppe close to forest (STE, grey), disturbed forest with regrowth of trees (DWIR, blue) and disturbed forest showing no regrowth of trees (DNOR, orange). n = 49, P values were calculated for differences between the arithmetic means (ns: p > 0.05; *: p ≤ 0.05; **: p ≤ 0.01; ***: p ≤ 0.001; ****: p ≤ 0.0001). Horizontal bars = medians, boxes = first and third quartiles, points = outliers, violins = data distributions.

Plant-available field capacity calculated by pedo-transfer functions from the literature (FC$_{pa,cal}$) and measured plant-available field capacity (FC$_{pa}$) did not match well, and the highest obtained R^2 was only 0.195 (see supplement Table_S1). We chose the pedo-transfer function of Gupta and Larson (1979), because of the wide range of soils used in their dataset, making it widely applicable. We assume that the mismatch with our measured data was due to disturbance of the samples during the transport from Mongolia to Germany, and due to high rock-fragment contents in many of our samples, creating several problems. For instance, there was a risk that rock fragments might have been hit and slightly moved by the cylinders, when these were hammered into the soil, and that moving rock fragments in turn pushed finer particles, thus slightly altering the pore-size distribution, the contribution of rock fragments to FC$_{pa}$ was neglected, and there was uncertainty in the calculation of rock-fragment content [vol.%] based on soil bulk density and an assumed rock density of 2.65 g cm^3. FC$_{pa,cal}$ [vol.%] of each horizon was transformed into plant-available water volume at field capacity (PAWV$_{FC}$) per square metre in the whole soil profile (Figure 8, left), and only in the uppermost 10 cm of the soils (Figure 8, right). Thereby, we assumed that PAWV$_{FC}$ stored in the whole profile is the relevant factor for mature trees, whereas PAWV$_{FC}$ stored in the uppermost 10 cm of the soils is crucial for the reestablishment of seedlings after forest disturbance.

19

360 There were no significant differences in PAWV$_{FC}$ of the whole soil profiles between the four vegetation categories (Figure 8, left). In contrast, PAWV$_{FC}$ in the uppermost 10 cm was significantly higher in soils under DWIR compared to soils under all other vegetation categories (Figure 8, right). Soils under FOR, STE and DNOR showed no significant difference in PAWV$_{FC}$ in their uppermost 10 cm. Soils under FOR exhibited a very wide range of PAWV$_{FC}$ in their upper most 10 cm.

Water repellency of topsoils under different vegetation categories did not show any differences (Fig. A2, appendix). Topsoil
365 samples from all vegetation categories included samples, on which the water drop only persisted for one or a few seconds, and samples on which the drop persisted for more than 1000 seconds.

4 Discussion

4.1 Chemical soil properties

In general, Siberian larch has low requirements with respect to chemical soil properties (Dylis, 1947). It can grow on a wide
370 range of soils and may colonise even rather fresh sediments (Timoshok and Skorokhodov, 2014). Siberian larch can also adapt to low nutrient availability by enhanced soil nutrient exploitation (Lebedev, 2012; Chernyshenko and Vasilyev, 2019). Most importantly, it needs nitrogen (Lebedev, 2010; Chernyshenko and Vasilyev, 2019), like many other larch species including *Larix gmelinii* (Schulze et al., 1995; Liang et al., 2014), *Larix kaempferi* (Leyton, 1956; Kayama et al., 2009) and hybrids such as *Larix x eurolepis* (Pâques, 1994). Also a lack in K and Mg may limit the growth of larch species on poor, sandy soils
375 (Leyton, 1956; Phu, 1975), whereas growth limitation by insufficient P supply has not yet been reported. Generally, differences in the vitality and growth of larch are more commonly caused by climatic or hydrological differences than by nutrient limitations (Fiedler et al., 1980; Stüber, 1998; Viers et al., 2013).

Because of the low nutrient requirements of Siberian larch and since we did not detect any significant differences in the chemical properties of soils under d̲isturbed forest w̲it̲h r̲egrowth of trees (DWIR) and under d̲isturbed forest showing n̲o
380 regrowth of trees (DNOR), we conclude that chemical soil properties are not responsible for the differences in post-disturbance regrowth of Siberian larch in our study area. The uppermost 10 cm of the soils under FOR had even significantly smaller N stocks and lower contents of exchangeable Ca, Mg and K than the uppermost 10 cm of the soils under DNOR. Nevertheless, saplings and young trees were growing in the FOR areas, which confirms that the nutrient supply of all analysed soils fulfilled the needs of Siberian larch. Also, nutrient stocks were similar or even higher compared to those reported from other Siberian
385 larch forests and from forests of other larch species (Kayama et al., 2009; Watanabe et al., 2012; Wang et al., 2014).

4.2 Physical soil properties and soil hydrology

Soils under DWIR had significantly more silt and clay, and thus higher plant-available field capacity than soils under DNOR, which were considerably sandier (Figure 4). As mean annual precipitation in Tosontsengel is only 200-250 mm, lack of water represents a major limitation for tree growth (Dulamsuren et al., 2011; Chenlemuge et al., 2015). Under these climatic

390 conditions, it is plausible that silt and clay content, and corresponding plant-available field capacity are key factors controlling the post-disturbance tree regrowth pattern. The similarity in silt and clay contents of soils under DNOR and soils under STE (no significant difference in Figure 4) points to a potential risk of DNOR sites to permanently shift to steppe vegetation. Such potential shift has already been predicted for the forest-steppe in the Khentey Mountains, Mongolia (Dulamsuren and Hauck, 2008; Dulamsuren et al., 2009).

395 Measured plant-available field capacities confirmed the difference between soils under DWIR and DNOR. Calculated $PAWV_{FC}$ further underscored the crucial role of soil water storage for post-disturbance tree regrowth under the given climatic conditions. With respect to $PAWV_{FC}$ of the whole soil profiles, the absence of any significant differences between the four vegetation categories (Figure 8, left) is in accordance with the fact that mature trees were originally able to grow on all of these north-facing slopes prior to a severe disturbance. With respect to the uppermost 10 cm of the soils, the significantly higher

400 $PAWV_{FC}$ under DWIR compared to soils under all other vegetation categories (Figure 8, right) highlights the importance of water storage in the uppermost centimetres for the re-establishment and survival of seedlings after severe forest disturbance, which is the precondition for post-disturbance forest recovery. The very wide $PAWV_{FC}$ range in the uppermost 10 cm of soils under FOR suggests that these FOR sites include both, sites where seedlings will be able to re-establish after severe disturbance, and sites where this won't be possible, which means that most likely no forest regrowth will take place, if once a severe forest

405 disturbance happens to these sites.

In the site-wise comparison, hydraulic conductivity tended to be higher in the uppermost horizons of soils under DWIR compared to their counterparts under DNOR. Trees may benefit from this difference for two reasons. Firstly, rapid infiltration through the uppermost horizons reduces evaporation loss. Secondly, grasses and herbs have a dense but shallow root system and compete with tree roots for water at shallow soil depth. As tree roots reach deeper down the soil, they benefit from rapid

410 water infiltration below the depth of the roots of grasses and herbs. Lange et al. (2015) carried out irrigation experiments on grass-dominated south-facing slopes and forest-dominated north-facing slopes in the Mongolian forest-steppe. On south-facing slopes, most of the water was either taken up by grass or evaporated, and the remaining water reached only 5 cm soil depth. On north-facing slopes, the water percolated down to the permafrost table. Although the contrasting exposition also affected this experiment, these results confirm the competitiveness of grasses for water in the upper soil horizons and the relevance of

415 soil hydraulic conductivity for tree growth in water-limited environments.

We did not detect a positive effect of permafrost on post-disturbance tree regrowth, as permafrost was neither encountered under DWIR nor under DNOR. This is in agreement with observations by Kopp et al. (2014), who reported absence of permafrost five years after severe forest fire. The same authors moreover measured increased soil moisture in soils of burned sites, compared to soils under forest, which they attributed to the absence of tree transpiration. In contrast, Park et al. (2009)

420 stated a decrease in soil moisture after fire and logging, arguing that evaporation loss from the bare soils and deterioration of physical soil properties exceed the decrease in transpiration. In our study area, we also observed rather decreased soil moisture at sites disturbed by fire and logging, compared to near-natural forest sites. An additional decline in soil moisture after fire can be induced by water repellency that may increase surface run off (DeBano, 2000; Mataix-Solera and Doerr, 2004). However,

we did not observe a significant difference in water repellency between the four vegetation categories, possibly because of the high frequency of fires in in our study area, and associated enhanced erosion (Goldammer, 2002; Hessl et al., 2012). As water repellency occurred irregularly across the whole study area, including DWIR and DNOR, it seemed to be not relevant for the post-disturbance tree recovery pattern in our study area.
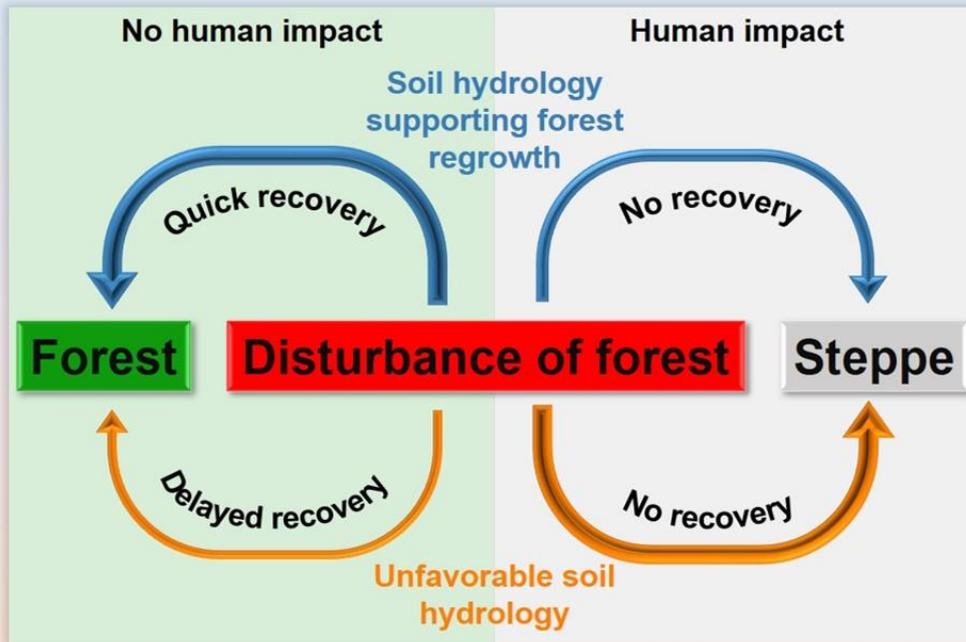
4.3 Further relevant environmental factors

Other factors besides soil hydrology that influence the post-disturbance tree regrowth pattern, include in particular relief and human activity. Relief-induced water gains in concave positions may support tree growth even where soil properties seem to be unfavourable. Similarly, water losses through divergence in convex positions may hamper tree growth, even where soil properties seem to be suitable. Also, small tree patches that survived a disturbance, can have a positive influence on post-disturbance tree regrowth. In our study area, we observed enhanced fructification of trees that had survived forest fires, initiating tree regrowth in belts around small tree patches that had persisted. We explain this observation by the shading of the remaining adult trees that reduces evaporation and creates a more even microclimate on the ground, and by increased availability of intact seeds in the direct surrounding of mature trees (Dugarjav, 2006).

In contrast, human activity, especially logging and pastoral pressure, may inhibit post-disturbance forest recovery (Khishigjargal et al., 2013; Dulamsuren et al., 2014; Khansaritoreh et al., 2017b). In particular, goats grazing in areas of burned forest or in forest stands that have previously been opened by partial logging, hamper the growth of seedlings and damage young trees (Sankey et al., 2006). Thus, human impact and soil hydrology are the two key factors controlling the post-disturbance tree regrowth pattern (Fig. 9). This is the outcome of this work, and relates to moderate and severe disturbances in our study area, which lead to deforested areas showing diverse tree-regrowth. Differences in tree-regrowth between moderate and severe disturbances were not detected. The observed low disturbances did not have considerable effects on the forests.

Loss of the shading by the forest canopy, of the forest microclimate and the insulating organic layer in turn lead to permafrost degradation. Also, the presently ongoing climate change accelerates permafrost decline in Mongolia. Thus, this essential soil water reservoir is likely to disappear (Sharkhuu and Sharkhuu, 2012). As the meltwater from the active layer above the permafrost table can support tree growth even at sites where soil water storage is below the threshold for tree growth, permafrost decline may also contribute to the decrease in forest area in the Mongolian forest-steppe. In some of our investigated sites, this has already happened.

Klinge et al. (2020) estimated that the potential forest distribution in the Khangai Mountains is three times larger than the actual forest area. This discrepancy indicates that forest fire and human activity already caused a considerable decline of forested areas.

Figure 9: Possible development pathways of disturbed forests in the Mongolian forest-steppe, as controlled by soil hydrology and human impact. Soil properties listed in dark blue = significant positive effect, light blue = non-significant positive effect, orange = significant negative effect.

5 Conclusions

This study showed that the post-disturbance regrowth pattern of forests in the central Mongolian forest-steppe, a highly sensitive, semi-arid landscape, is largely controlled by soil hydrology. With respect to our hypotheses established in the beginning, we conclude that:

1) Differences in post-disturbance tree regrowth depend mainly on the texture of the uppermost soil horizons. Loamy soils have high plant-available field capacity and are thus able to store sufficient amounts of water for post-disturbance re-establishment of seedlings as a precondition for forest regrowth. In contrast, sandy soils cannot store enough water for the re-establishment of seedlings and subsequent recovery of tree vegetation under the present environmental conditions.

2) Post-disturbance tree regrowth may be supported by higher hydraulic conductivity in the uppermost soil horizons, as rapid percolation through the upper soil horizons reduces evaporation loss. In addition, trees benefit from the reduced competition for water with grasses and herbs that results from rapid water percolation into the subsoil.

23

3) Nutrient limitation is not relevant for the uneven post-disturbance tree regrowth pattern in our study area, as the dominant tree species, Siberian larch, has rather low nutrient requirements.

470 4) Meltwater from the active layer above the permafrost table provides additional water for near-natural forests. However, it cannot be a relevant factor for the uneven post-disturbance regrowth pattern of Siberian larch in our study area, because permafrost was encountered neither under disturbed forests with nor without tree regrowth.

Under the given climatic conditions, water limitation is the predominant factor controlling tree growth in the semi-arid Mongolian forest-steppe. Therefore, even small differences in soil properties that lead to an increase in the amount of plant-475 available water, can be decisive for post-disturbance tree regrowth.

Disturbances by severe fire or clear-cutting result in loss of permafrost and thus loss of an additional water reservoir during summer. Such additional water source can be critical at sites, where soil water storage alone is slightly below the threshold for tree growth. Therefore, such sites are particularly prone to an irreversible shift from forest to steppe after strong disturbance, involving loss of permafrost. Moreover, we expect that many sites where soil hydrology allows for post-disturbance tree 480 regrowth under the present climatic conditions, will lose their ability for post-disturbance forest recovery in the course of the ongoing climate change, as the present conditions are very close to the threshold for forest growth, and already a minor change may lead to a fall below this threshold.

Climate projections predict that the decrease of permafrost will continue, and drought events will become both more frequent and more intensive. At the same time, it seems unlikely that the pressure on forests in the Mongolian forest-steppe by fire, 485 logging and grazing will decrease, unless explicit and effective measures are taken. Consequences of this unfavourable interplay will most likely include a decrease in the growth rates of trees, and a further considerable and irreversible decline of forested area. Therefore, regulation of human impact on the forests in the Mongolian forest-steppe is mandatory, if a further irreversible loss of forest area shall be avoided.

6 Appendix A

Table A1: General information on the soil profiles. Abbreviations are according to the Guidelines for Soil Description (Jahn et al., 2006). *: If permafrost is present, the depth of the permafrost table equals the profile depth.
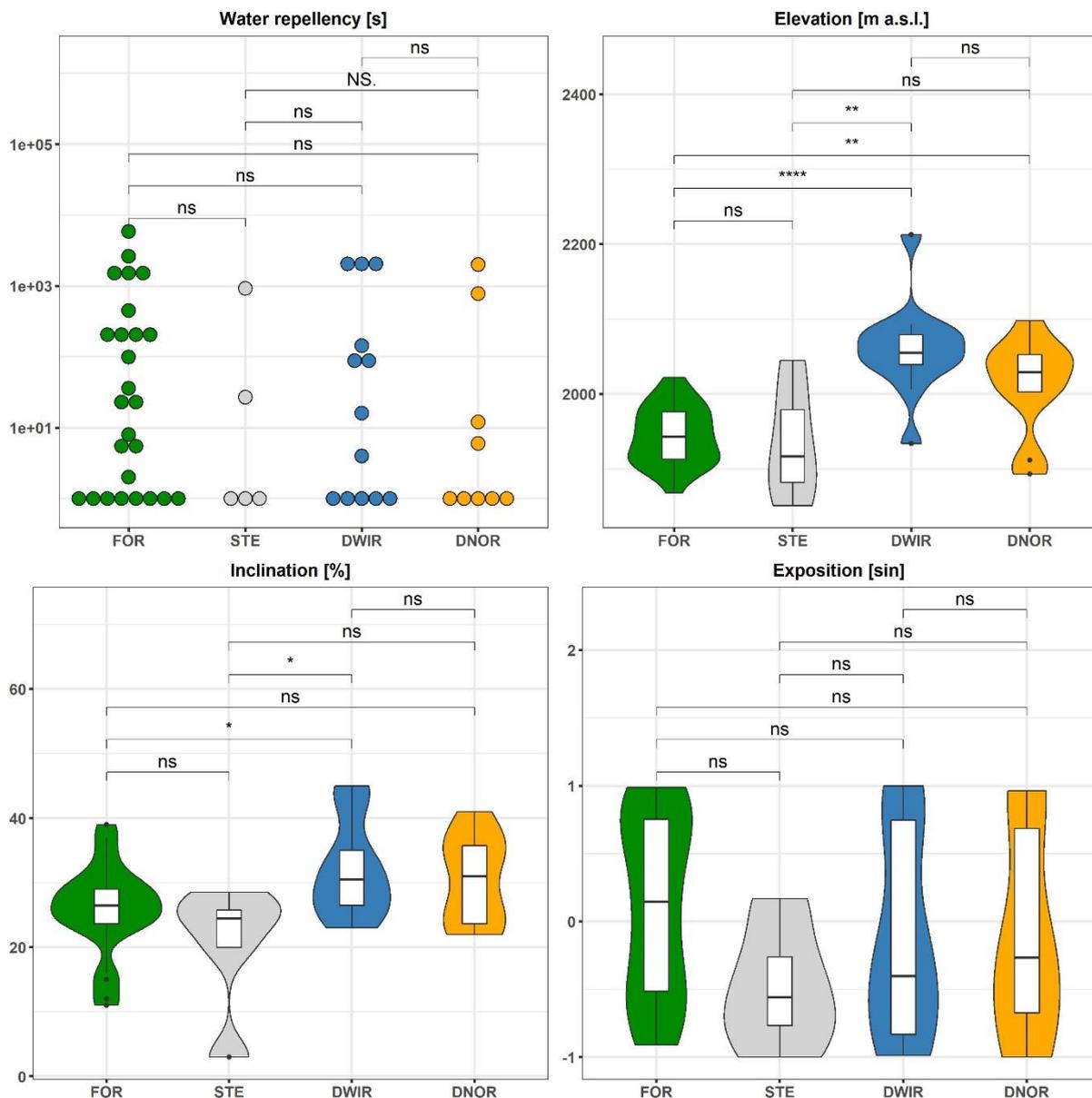
Vegeta tion catego ry	Pro file ID	Coordi nates N	Coordi nates E	Eleva tion [m a.s.l.]	Inclin ation [%]	Expo sition [°]	Bedro ck	Main sedi ment type	Penda nts on rock fragme nts	Profil e dept h [cm]	Prese nce of Perm afrost *	Distur bance by fire	Distur bance by loggin g	Soil type [based on WRB]
FOR	1	48° 38.681'	98° 22.141'	1915	24.5	320	granite	sand sheet	no	165	yes	no	no	Eutric **Cambisol** (Katoarenic, Bathygelic, Epiloamic, Nechic, Ochric, Endoraptic)
FOR	2	48° 38.700'	98° 22.034'	1907	26.5	340	granite	sand sheet	no	140	yes	no	no	Eutric **Cambisol** (Katoarenic, Bathygelic, Amphiloamic, Nechic, Ochric)
STE	3	48° 38.929'	98° 22.122'	1882	28.5	301	granite	bedro ck	no	90	no	no	no	Skeletic Cambic Endoleptic **Phaeozem** (Amphiarenic, Epiloamic, Nechric)
STE	4	48° 38.377'	98° 22.202'	1917	25.75	292	granite	colluv ium	no	90	no	no	no	Endoskeletic **Phaeozem** (Amphiarenic, Colluvic, Epiloamic, Nechric, Epiraptic)
STE	5	48° 38.736'	98° 21.853'	1851	20	307	granite	colluv ium	no	110	no	no	no	Endoskeletic **Chernozem** (Katoarenic, Cambic, Colluvic, Amphiloamic, Amphiraptic)
STE	6	48° 38.216'	98° 22.408'	1979	24.5	300	granite/ gneiss	slope depos it	no	120	no	no	no	Endoskeletic Endoleptic **Phaeozem** (Katoarenic, Colluvic, Epiloamic, Nechric, Epiraptic)
FOR	7	48° 38.181'	98° 22.487'	2007	31	304	granite/ gneiss	sand sheet	no	105	no	no	low	Eutric Endoskeletic **Cambisol** (Katoarenic, Epiloamic, Nechic, Ochric, Epiraptic)
FOR	8	48° 38.206'	98° 22.511'	2022	32	305	granite/ gneiss	sand sheet	no	120	no	no	low	Eutric Endoskeletic **Cambisol** (Katoarenic, Amphiloamic, Nechic, Ochric, Endoraptic)
FOR	9	48° 38.770'	98° 22.074'	1868	16	301	granite	sand sheet	no	180	yes	no	moder ate	Cambic **Phaeozem** (Katoarenic, Colluvic, Katoloamic, Nechic, Endoraptic, Bathyprotocalcic, Bathygleyic, Bathyturbic)
FOR	10	48° 38.748'	98° 22.169'	1900	26.5	303	granite	slope depos it	no	100	no	no	moder ate	Haplic **Phaeozem** (Endoarenic, Colluvic, Amphiloamic, Nechric, Amphiraptic)

Vegetation category	Profile ID	Coordinates N	Coordinates E	Elevation [m a.s.l.]	Inclination [%]	Exposition [°]	Bedrock	Main sediment type	Pendants on rock fragments	Profile depth [cm]	Presence of Permafrost *	Disturbance by fire	Disturbance by logging	Soil type [based on WRB]
FOR	11	48° 37.766'	98° 21.215'	1938	23.5	335	granite/ gneiss	slope deposit	manganese	60	yes	no	no	Endoskeletic Cambic Folic Reductaquic **Cryosol** (Epiarenic, Eutric, Amphiloamic, Nechic, Ochric, Epiraptic)
FOR	12	48° 37.775'	98° 21.277'	1943	28.5	317	granite/ gneiss	slope deposit	no	80	yes	no	no	Endoskeletic Folic Reductaquic **Cryosol** (Amphiarenic, Eutric, Epiloamic, Nechic, Ochric, Amphiraptic)
FOR	13	48° 37.258'	98° 21.517'	1974	27.5	335	granite/ gneiss	slope deposit	manganese	60	yes	no	no	Endoskeletic Folic Reductaquic **Cryosol** (Eutric, Loamic, Nechic, Ochric, Epiraptic)
FOR	14	48° 37.322'	98° 21.624'	1969	27	326	granite/ gneiss	slope deposit	no	80	yes	no	no	Endoskeletic Folic **Cryosol** (Epiarenic, Eutric, Amphiloamic, Nechic, Ochric, Epiraptic)
FOR	15	48° 37.728'	98° 21.233'	1947	25	324	granite/ gneiss	slope deposit	manganese	94	yes	no	no	Endoskeletic Cambic Folic Reductaquic **Cryosol** (Amphiarenic, Eutric, Amphiloamic, Nechic, Ochric, Epiraptic)
FOR	16	48° 37.787'	98° 21.210'	1913	23.5	357	granite/ gneiss	slope deposit	manganese	66	yes	no	low	Cambic Folic Reductaquic **Cryosol** (Amphiarenic, Eutric, Amphiloamic, Nechic, Ochric, Epiraptic)
FOR	17	48° 37.816'	98° 21.208'	1908	22	359	granite/ gneiss	slope deposit	no	80	yes	no	low	Endoskeletic Cambic Reductaquic **Cryosol** (Endoarenic, Eutric, Epiloamic, Nechic, Ochric, Amphiraptic)
FOR	18	48° 37.755'	98° 21.280'	1951	34.5	351	granite/ gneiss	slope deposit	manganese	100	yes	no	no	Endoskeletic Cambic Reductaquic **Cryosol** (Epiarenic, Eutric, Amphiloamic, Nechic, Ochric, Epiraptic)
FOR	19	48° 37.799'	98° 21.268'	1930	30	358	granite/ gneiss	slope deposit	manganese	80	yes	no	no	Endoskeletic Folic Reductaquic **Cryosol** (Eutric, Loamic, Nechic, Ochric, Epiraptic)
FOR	20	48° 37.825'	98° 21.271'	1914	24	1	granite/ gneiss	slope deposit	no	65	yes	no	no	Endoskeletic Cambic Folic Reductaquic **Cryosol** (Endoarenic, Eutric, Anoloamic, Nechic, Ochric, Endoraptic)
FOR	21	48° 37.700'	98° 21.276'	1990	39	315	granite/ gneiss	slope deposit	no	90	yes	no	no	Endoskeletic Reductaquic **Cryosol** (Amphiarenic, Eutric, Amphiloamic, Nechic, Ochric, Epiraptic)
FOR	22	48° 37.830'	98° 21.208'	1900	11	334	granite/ gneiss	slope deposit	no	90	yes	no	low	Endoskeletic Folic Reductaquic **Cryosol** (Endoarenic, Eutric,

Vegetation category	Profile ID	Coordinates N	Coordinates E	Elevation [m a.s.l.]	Inclination [%]	Exposition [°]	Bedrock	Main sediment type	Pendants on rock fragments	Profile depth [cm]	Presence of Permafrost *	Disturbance by fire	Disturbance by logging	Soil type [based on WRB]
														Amphiloamic, Nechic, Ochric, Amphiraptic)
FOR	23	48° 37.736'	98° 21.290'	1977	37	345	granite/ gneiss	slope deposit	no	100	yes	no	no	Endoskeletic Reductaquic **Cryosol** (Amphiarenic, Eutric, Epiloamic, Nechic, Ochric, Epiraptic)
FOR	24	48° 37.843'	98° 21.256'	1908	12	352	granite/ gneiss	slope deposit	no	90	yes	no	low	Endoskeletic Folic Reductaquic **Cryosol** (Endoarenic, Eutric, Amphiloamic, Nechic, Ochric, Epiraptic)
FOR	25	48° 37.649'	98° 21.231'	1994	28.5	336	granite/ gneiss	slope deposit	no	70	no	no	no	Eutric Endoskeletic **Cambisol** (Gelic, Gelistagnic, Loamic, Nechric, Ochric, Epiraptic)
FOR	26	48° 37.669'	98° 21.199'	1982	29	346	granite/ gneiss	slope deposit	no	70	yes	no	no	Endoskeletic Folic Reductaquic **Cryosol** (Epiarenic, Eutric, Amphiloamic, Nechic, Ochric, Epiraptic)
FOR	27	48° 37.697'	98° 21.184'	1977	29	356	granite/ gneiss	slope deposit	no	58	yes	no	no	Cambic Folic **Cryosol** (Eutric, Loamic, Nechic, Ochric, Epiraptic)
FOR	28	48° 37.725'	98° 21.161'	1957	24.5	352	granite/ gneiss	slope deposit	no	80	yes	no	no	Endoskeletic Folic Reductaquic **Cryosol** (Amphiarenic, Eutric, Amphiloamic, Nechic, Ochric, Epiraptic)
FOR	29	48° 37.768'	98° 21.135'	1943	25.5	353	granite/ gneiss	slope deposit	no	80	yes	no	no	Endoskeletic Folic Reductaquic **Cryosol** (Epiarenic, Eutric, Amphiloamic, Nechic, Ochric, Epiraptic)
FOR	30	48° 37.787'	98° 21.127'	1915	15	351	granite/ gneiss	slope deposit	no	70	yes	no	low	Endoskeletic Cambic Folic Reductaquic **Cryosol** (Eutric, Loamic, Nechic, Ochric, Epiraptic)
DNOR	31	48° 27.636'	98° 13.686'	2046	22	316	granite/ gneiss	slope deposit	calcium carbonate	100	no	severe	moderate	Eutric Endoskeletic **Cambisol** (Endoarenic, Amphiloamic, Nechric, Ochric, Amphiraptic)
DNOR	32	48° 27.640'	98° 13.730'	2055	25.5	344	granite/ gneiss	slope deposit	calcium carbonate	80	no	severe	moderate	Eutric Endoskeletic **Cambisol** (Endoarenic, Colluvic, Epilomic, Nechric, Ochric, Epiraptic)
DWIR	33	48° 27.549'	98° 13.576'	2055	25	312	granite/ gneiss	slope deposit	calcium carbonate	80	no	severe	moderate	Eutric Endoskeletic C**ambisol** (Colluvic, Loamic, Nechric, Ochric, Epiraptic)

Vegetation category	Profile ID	Coordinates N	Coordinates E	Elevation [m a.s.l.]	Inclination [%]	Exposition [°]	Bedrock	Main sediment type	Pendants on rock fragments	Profile depth [cm]	Presence of Permafrost*	Disturbance by fire	Disturbance by logging	Soil type [based on WRB]
DWIR	34	48° 27.595'	98° 13.723'	2079	32.5	332	granite/ gneiss	slope deposit	manganese, calcium carbonate	90	no	severe	moderate	Eutric Endoskeletic **Cambisol** (Protocalcic, Colluvic, Loamic, Nechric, Ochric, Amphiraptic)
DWIR	35	48° 27.597'	98° 10.886'	2077	26.5	322	granite/ gneiss	slope deposit	no	90	no	severe	moderate	Eutric Endoskeletic **Cambisol** (Loamic, Nechric, Ochric, Epiraptic)
DWIR	36	48° 27.609'	98° 10.914'	2069	29.5	320	granite/ gneiss	slope deposit	no	100	no	severe	moderate	Eutric Endoskeletic **Cambisol** (Loamic, Nechric, Ochric, Epiraptic)
DWIR	37	48° 28.784'	98° 19.246'	2088	35	324	granite/ gneiss	slope deposit	no	110	no	severe	moderate	Eutric Endoskeletic **Cambisol** (Amphiarenic, Colluvic, Epiloamic, Nechric, Ochric, Epiraptic)
DNOR	38	48° 28.790'	98° 19.074'	2004	41	328	granite/ gneiss	colluvium	no	100	no	severe	moderate	Endoskeletic **Phaeozem** (Amphiarenic, Colluvic, Epiloamic, Nechric, Ochric, Amphiraptic)
DNOR	39	48° 28.732'	98° 18.980'	2018	36	328	granite/ gneiss	slope deposit	calcium carbonate	115	no	severe	severe	Eutric Endoskeletic **Cambisol** (Amphiarenic, Colluvic, Epiloamic, Nechric, Ochric, Amphiraptic)
DNOR	40	48° 28.335'	98° 19.140'	2040	36.5	320	granite/ gneiss	slope deposit	manganese, calcium carbonate	100	no	severe	moderate	Eutric Endoskeletic **Cambisol** (Amphiarenic, Colluvic, Epiloamic, Nechric, Ochric, Amphiraptic)
DWIR	41	48° 28.345'	98° 19.228'	2053	42.5	330	granite/ gneiss	slope deposit	calcium carbonate	110	no	severe	moderate	Eutric Endoskeletic **Cambisol** (Amphiarenic, Colluvic, Epiloamic, Nechric, Ochric, Amphiraptic)
DNOR	42	48° 33.181'	98° 13.362'	1893	23	330	granite	slope deposit	no	110	no	no	severe	Haplic **Kastanozem** (Amphiarenic, Cambic, Colluvic, Epiloamic, Nechric, Epiraptic)
DNOR	43	48° 24.506'	98° 18.295'	1912	35	17	granite	slope deposit	no	125	no	no	severe	Skeletic **Phaeozem** (Katoarenic, Colluvic, Amphiloamic, Nechric, Amphiraptic)
DWIR	44	48° 48.525'	98° 19.850'	2093	25.5	320	granite/ gneiss	slope deposit	no	100	no	severe	severe	Eutric Endoskeletic **Cambisol** (Amphiarenic, Epiloamic, Nechric, Ochric, Amphiraptic)
DNOR	45	48° 48.371'	98° 19.351'	2059	23	324	granite/ gneiss	slope deposit	no	90	no	severe	severe	Eutric Endoskeletic **Cambisol** (Amphiarenic, Epiloamic, Nechric, Ochric, Epiraptic)

Vegetation category	Profile ID	Coordinates N	Coordinates E	Elevation [m a.s.l.]	Inclination [%]	Exposition [°]	Bedrock	Main sediment type	Pendants on rock fragments	Profile depth [cm]	Presence of Permafrost*	Disturbance by fire	Disturbance by logging	Soil type [based on WRB]
DNOR	46	48° 48.400'	98° 19.136'	2002	28	330	granite/ gneiss	slope deposit	manganese	105	no	severe	severe	Eutric Endoskeletic **Cambisol** (Katoarenic, Epiloamic, Nechric, Ochric, Amphiraptic)
DWIR	47	48° 52.582'	98° 19.482'	2006	32.5	315	granite/ gneiss	bedrock	manganese	80	no	moderate	moderate	Eutric Endoskeletic Endoleptic **Cambisol** (Amphiarenic, Amphiloamic, Nechric, Ochric, Epiraptic)
STE	48	48° 16.462'	98° 21.224'	2045	3	305	granite	slope deposit	calcium carbonate	130	no	no	no	Haplic **Kastanozem** (Cambic, Loamic, Amphiraptic)
DWIR	49	48° 16.438'	98° 20.856'	2043	26.5	325	granite	slope deposit	manganese	90	no	severe	moderate	Eutric Endoskeletic **Cambisol** (Amphiarenic, Epiloamic, Nechric, Ochric, Epiraptic)
DWIR	50	48° 22.427'	98° 38.329'	2039	23	357	granite	slope deposit	no	105	no	severe	moderate	Endoskeletic **Phaeozem** (Katoarenic, Colluvic, Amphiloamic, Nechric, Amphiraptic)
DNOR	51	48° 22.293'	98° 38.313'	2098	34	4	granite	slope deposit	no	110	no	severe	moderate	Endoskeletic **Phaeozem** (Katoarenic, Colluvic, Amphiloamic, Nechric, Amphiraptic)
DWIR	52	48° 22.113'	98° 38.247'	2213	30.5	355	granite	bedrock	no	52	no	severe	no	Endoskeletic Endoleptic **Phaeozem** (Loamic, Nechric, Epiraptic)
DWIR	53	48° 41.506'	98° 27.930'	1934	45	290	gneiss	slope deposit	manganese	95	no	moderate	moderate	Skeletic Endoleptic **Phaeozem** (Amphiarenic, Epiloamic, Nechric, Epiraptic)
DWIR	54	48° 41.471'	98° 28.073'	2033	44.5	291	gneiss	slope deposit	manganese	75	no	moderate	moderate	Endoskeletic Endoleptic **Phaeozem** (Amphiarenic, Epiloamic, Nechric, Epiraptic)

Figure A2: Scatter plots for water repellency (expressed as water drop infiltration time in seconds; n = 53), and violin plots and boxplots elevation (n = 54), inclination (n = 54), and exposition (n = 54) of the soils under the four vegetation categories near-natural forest (FOR, green), steppe close to forest (STE, grey), disturbed forest with regrowth of trees (DWIR, blue) and disturbed forest showing no regrowth of trees (DNOR, orange). P values were calculated for differences between the arithmetic means (NS.: p = 1; ns: p > 0.05; *: p ≤ 0.05; **: p ≤ 0.01; ***: p ≤ 0.001; ****: p ≤ 0.0001). Horizontal bars = medians, boxes = first and third quartiles, points = outliers, violins = data distributions.

Code/Data availability:

See supplementary material (data.xlsx).

30

Authors contribution:

Competing interests:

The authors declare that they have no conflict of interest.

Acknowledgements

References

Academy of Sciences of Mongolia, Academy of Sciences of USSR: National Atlas of the Peoples Republic of Mongolia,
520 Ulaanbaatar, Moscow, 1990.

Albenskiy, A. V., Krylov, G. V., Logginov, B. J., and Scherlin, J. D.: Usage of fast growing breeds in field protection forest
cultivation (in Russian), Moskow, 1956.

Allen, C. D., Macalady, A. K., Chenchouni, H., Bachelet, D., McDowell, N., Vennetier, M., Kitzberger, T., Rigling, A.,
Breshears, D. D., Hogg, E. H., Gonzalez, P., Fensham, R., Zhang, Z., Castro, J., Demidova, N., Lim, J.-H., Allard, G.,
525 Running, S. W., Semerci, A., and Cobb, N.: A global overview of drought and heat-induced tree mortality reveals
emerging climate change risks for forests, Forest Ecology and Management, 259, 660–684,
https://doi.org/10.1016/j.foreco.2009.09.001, 2010.

Amoozegar, A. and Warrick, A. W.: Hydraulic Conductivity of Saturated Soils: Field Methods, American Society of
Agronomy-Soil Science Society of America, 735–770, 1986.

530 Batima, P., Natsagdorj, L., Gombluudev, P., and Erdenetsetseg, B.: Observed climate change in Mongolia, Assessments of Impacts and Adaptations of Climate Change, 1–26, 2005.

Beaudette, D. E., Roudier, P., and O'Geen, A. T.: Algorithms for quantitative pedology: A toolkit for soil scientists, Computers & Geosciences, 52, 258–268, https://doi.org/10.1016/j.cageo.2012.10.020, 2013.

Bonan, G. B. and Shugart, H. H.: Environmental Factors and Ecological Processes in Boreal Forests, Annual Review of 535 Ecology, Evolution, and Systematics, 20, 1–28, 1989.

Chenlemuge, T., Schuldt, B., Dulamsuren, C., Hertel, D., Leuschner, C., and Hauck, M.: Stem increment and hydraulic architecture of a boreal conifer (Larix sibirica) under contrasting macroclimates, Trees, 29, 623–636, https://doi.org/10.1007/s00468-014-1131-x, 2015.

Chernyshenko, O. V. and Vasilyev, S. B.: Mineral nutrition specificity of coniferous trees on industrial waste discharge of 540 Egorievsk phosphorite deposit (in Russian), Forestry Bulletin, 46–53, https://doi.org/10.18698/2542-1468-2019-5-46-53, 2019.

Churakova, O. V., Shashkin, A. V., Siegwolf, R. T. W., Spahni, R., Launois, T., Saurer, M., Bryukhanova, M. V., Benkova, A. V., Kuptsova, A. V., Peylin, P., Vaganov, E. A., Masson-Delmotte, V., and Roden, J.: Application of eco-physiological models to the climatic interpretation of $\delta 13C$ and $\delta 18O$ measured in Siberian larch tree-rings, 545 Dendrochronologia, 39, 51–59, https://doi.org/10.1016/j.dendro.2015.12.008, 2016.

Dashkhuu, D., Kim, J. P., Chun, J. A., and Lee, W.-S.: Long-term trends in daily temperature extremes over Mongolia, Weather and Climate Extremes, 8, 26–33, https://doi.org/10.1016/j.wace.2014.11.003, 2015.

Dashtseren, A., Ishikawa, M., Iijima, Y., and Jambaljav, Y.: Temperature Regimes of the Active Layer and Seasonally Frozen Ground under a Forest-Steppe Mosaic, Mongolia, Permafrost and Periglacial Processes, 25, 295–306, 550 https://doi.org/10.1002/ppp.1824, 2014.

DeBano, L.: The role of fire and soil heating on water repellency in wildland environments: a review, Journal of Hydrology, 231-232, 195–206, https://doi.org/10.1016/S0022-1694(00)00194-3, 2000.

Doerr, S. H.: On standardizing the 'Water Drop Penetration Time' and the 'Molarity of an Ethanol Droplet' techniques to classify soil hydrophobicity: A case study using medium textured soils, Earth Surface Processes and Landforms, 23, 555 663–668, https://doi.org/10.1002/(SICI)1096-9837(199807)23:7<663:AID-ESP909>3.0.CO;2-6, 1998.

Doerr, S. H., Shakesby, R. A., and Walsh, R.: Soil water repellency: its causes, characteristics and hydro-geomorphological significance, Earth-Science Reviews, 51, 33–65, https://doi.org/10.1016/S0012-8252(00)00011-8, 2000.

Dugarjav, C.: Larch forests of Mongolia (in Mongolian), Bembi San, Ulan Bator, 2006.

Dulamsuren, C. and Hauck, M.: Spatial and seasonal variation of climate on steppe slopes of the northern Mongolian 560 mountain taiga, Grassland Science, 54, 217–230, https://doi.org/10.1111/j.1744-697X.2008.00128.x, 2008.

Dulamsuren, C., Khishigjargal, M., Leuschner, C., and Hauck, M.: Response of tree-ring width to climate warming and selective logging in larch forests of the Mongolian Altai, Journal of Plant Ecology, 7, 24–38, https://doi.org/10.1093/jpe/rtt019, 2014.

Dulamsuren, C., Hauck, M., Leuschner, H. H., and Leuschner, C.: Climate response of tree-ring width in Larix sibirica growing in the drought-stressed forest-steppe ecotone of northern Mongolia, Annals of Forest Science, 68, 275–282, https://doi.org/10.1007/s13595-011-0043-9, 2011.

Dulamsuren, C., Hauck, M., and Leuschner, C.: Recent drought stress leads to growth reductions in Larix sibirica in the western Khentey, Mongolia, Global Change Biology, 95, 3024-3035, https://doi.org/10.1111/j.1365-2486.2009.02147.x, 2010.

Dulamsuren, C., Hauck, M., Bader, M., Osokhjargal, D., Oyungerel, S., Nyambayar, S., Runge, M., and Leuschner, C.: Water relations and photosynthetic performance in Larix sibirica growing in the forest-steppe ecotone of northern Mongolia, Tree physiology, 29, 99–110, https://doi.org/10.1093/treephys/tpn008, 2009.

Dylis, N. V.: Siberian larch (in Russian), Moskow, 1947.

Fiedler, H. J., Hunger, W., Müller, K., and Skodawessely, K.: Zu den Beziehungen zwischen Boden, Ernährungszustand und Wuchsleistung bei Lärche (Larix decidua Mill.) (in German), Flora, 170, 1–19, https://doi.org/10.1016/S0367-2530(17)31187-8, 1980.

Goldammer, J. G.: Fire Situation in Mongolia (IFFN No. 26) | GFMC, http://gfmc.online/iffn/country/mn/mn_11.html, last access: 14 October 2019, 2002.

Grunert, J., Lehmkuhl, F., and Walther, M.: Paleoclimatic evolution of the Uvs Nuur basin and adjacent areas (Western Mongolia), Quaternary International, 65-66, 171–192, https://doi.org/10.1016/S1040-6182(99)00043-9, 2000.

Gupta, S. C. and Larson, W. E.: Estimating soil water retention characteristics from particle size distribution, organic matter percent, and bulk density, Water Resources Research, 15, 1633–1635, https://doi.org/10.1029/WR015i006p01633, 1979.

Haase, G.: Die Höhenstufen der Böden im Changai (MVR) (in German), Zeitschrift für Pflanzenernährung, Düngung, Bodenkunde, 102, 113–127, https://doi.org/10.1002/jpln.19631020205, 1963.

Hais, M., Chytrý, M., and Horsák, M.: Exposure-related forest-steppe: A diverse landscape type determined by topography and climate, Journal of Arid Environments, 135, 75–84, https://doi.org/10.1016/j.jaridenv.2016.08.011, 2016.

Hessl, A. E., Brown, P., Byambasuren, O., Cockrell, S., Leland, C., Cook, E. R., Nachin, B., Pederson, N., Saladyga, T., and Suran, B.: Fire and climate in Mongolia (1532-2010 Common Era), Geophysical Research Letters, 43, 6519–6527, https://doi.org/10.1002/2016GL069059, 2016.

Hessl, A. E., Ariya, U., Brown, P., Byambasuren, O., Green, T. R., Jacoby, G. C., Sutherland, E. K., Nachin, B., Maxwell, R. S., Pederson, N., Grandpré, L. de, Saladyga, T., and Tardif, J. C.: Reconstructing fire history in central Mongolia from tree-rings, International Journal of Wildland Fire, 21, 86, https://doi.org/10.1071/WF10108, 2012.

Hilbig, W.: Zur Problematik der ursprünglichen Waldverbreitung in der Mongolischen Volksrepublik Ergebnisse der Mongolisch - Deutschen Biologischen Expeditionen seit 1962, Nr. 181 (in German), Flora, 179, 1–15, https://doi.org/10.1016/S0367-2530(17)30213-X, 1987.

Ishikawa, M., Sharkhuu, N., Zhang, Y., Kadota, T., and Ohata, T.: Ground Thermal and Moisture Conditions at the Southern Boundary of Discontinuous Permafrost, Mongolia, Permafrost and Periglacial Processes, 16, 209–216, https://doi.org/10.1002/ppp.483, 2005.

IUSS Working Group WRB: World reference base for soil resources 2014: International soil classification system for naming soils and creating legends for soil maps, World soil resources reports, 106, FAO, Rome, 181 pp., 2015.

Jahn, R., Blume, H.-P., Asio, V. B., Spaargaren, O., and Schad, P. (Eds.): Guidelines for soil description, 4., [rev.] ed., FAO, Rome, 97 pp., 2006.

Kapper, O. G.: Conifer Species (in Russian): Forestry Characteristics, Moskow, Leningrad, 1954.

Kassambara, A.: ggpubr: 'ggplot2' Based Publication Ready Plots, 2019.

Kassambara, A. and Mundt, F.: factoextra: Extract and Visualize the Results of, 2019.

Kayama, M., Makoto, K., Nomura, M., Satoh, F., and Koike, T.: Nutrient dynamics and carbon partitioning in larch seedlings (Larix kaempferi) regenerated on serpentine soil in northern Japan, Landscape and Ecological Engineering, 5, 125–135, https://doi.org/10.1007/s11355-009-0069-4, 2009.

Khansaritoreh, E., Dulamsuren, C., Klinge, M., Ariunbaatar, T., Bat-Enerel, B., Batsaikhan, G., Ganbaatar, K., Saindovdon, D., Yeruult, Y., Tsogtbaatar, J., Tuya, D., Leuschner, C., and Hauck, M.: Higher climate warming sensitivity of Siberian larch in small than large forest islands in the fragmented Mongolian forest steppe, Global Change Biology, 23, 3675–3689, https://doi.org/10.1111/gcb.13750, 2017a.

Khansaritoreh, E., Eldarov, M., Ganbaatar, K., Saindovdon, D., Leuschner, C., Hauck, M., and Dulamsuren, C.: Age structure and trends in annual stem increment of Larix sibirica in two neighboring Mongolian forest–steppe regions differing in land use history, Trees, 31, 1973–1986, https://doi.org/10.1007/s00468-017-1601-z, 2017b.

Kharuk, V. I., Ranson, K. J., and Dvinskaya, M. L.: Wildfires dynamic in the larch dominance zone, Geophysical Research Letters, 35, 1–6, https://doi.org/10.1029/2007GL032291, 2008.

Khishigjargal, M., Dulamsuren, C., Lkhagvadorj, D., Leuschner, C., and Hauck, M.: Contrasting responses of seedling and sapling densities to livestock density in the Mongolian forest-steppe, Plant Ecology, 214, 1391–1403, https://doi.org/10.1007/s11258-013-0259-x, 2013.

Klinge, M. and Lehmkuhl, F.: Geomorphology of the Tsetseg Nuur basin, Mongolian Altai – lake development, fluvial sedimentation and aeolian transport in a semi-arid environment, Journal of Maps, 9, 361–366, https://doi.org/10.1080/17445647.2013.783513, 2013.

Klinge, M., Schneider, F., Dulamsuren, C., Arndt, K., Bayarsaikhan, U., and Sauer, D.: Interrelations between vegetation, natural and anthropogenic disturbances, and discontinuous permafrost in the forest-steppe of central Mongolia, under revision, Earth Surface Processes and Landforms, 2021.

Klinge, M., Dulamsuren, C., Schneider, F., Erasmi, S., Hauck, M., Bayarsaikhan, U., and Sauer, D.: Modelled potential forest area in the forest-steppe of central Mongolia is about three times of actual forest area, Biogeosciences, Preprint, https://doi.org/10.5194/bg-2020-13, 2020.

630   Klinge, M., Dulamsuren, C., Erasmi, S., Karger, D. N., and Hauck, M.: Climate effects on vegetation vitality at the treeline of boreal forests of Mongolia, Biogeosciences, 15, 1319–1333, https://doi.org/10.5194/bg-15-1319-2018, 2018.

Kopp, B. J., Minderlein, S., and Menzel, L.: Soil Moisture Dynamics in a Mountainous Headwater Area in the Discontinuous Permafrost Zone of northern Mongolia, Arctic, Antarctic, and Alpine Research, 46, 459–470, https://doi.org/10.1657/1938-4246-46.2.459, 2014.

635   Krasnoshchekov, Y. N.: Soils and the Soil Cover of Mountainous Tundra and Forest Landscapes in the Central Khangai of Mongolia, Eurasian Soil Science, 43, 117–126, https://doi.org/10.1134/S1064229310020018, 2010.

Krasnoshchekov, Y. N.: Soil cover of mountain forests in the East Khubsugul region of Mongolia, Eurasian Soil Science, 41, 694–703, https://doi.org/10.1134/S106422930807003X, 2008.

Lange, J., Kopp, B. J., Bents, M., and Menzel, L.: Tracing variability of run-off generation in mountainous permafrost of
640   semi-arid north-eastern Mongolia, Hydrological Processes, 29, 1046–1055, https://doi.org/10.1002/hyp.10218, 2015.

Lê, S., Josse, J., and Husson, F.: FactoMineR: An R Package for Multivariate Analysis, Journal of Statistical Software, 25, 1–18, 2008.

Lebedev, E. V.: Quantitative Measurements of Net Productivity of Photosynthesis, Mineral Nutrition and Biological Productivity of Larix sibirica During Ontogenesis in the Areal of Southern Altai (in Russian), Herald of Altai state
645   agricultural university, 12, 61–66, 2012.

Lebedev, E. V.: Impact of nitrogen forms on photosynthesis, mineral nutrition and biological productivity of plants as Siberian larch and European spruce (in Russian), Forestry Bulletin, 6, 14–18, 2010.

Lehmkuhl, F. and Haselein, F.: Quaternary paleoenvironmental change on the Tibetan Plateau and adjacent areas (Western China and Western Mongolia), Quaternary International, 65-66, 121–145, https://doi.org/10.1016/S1040-
650   6182(99)00040-3, 2000.

Lehmkuhl, F., Hilgers, A., Fries, S., Hülle, D., Schlütz, F., Shumilovskikh, L., Felauer, T., and Protze, J.: Holocene geomorphological processes and soil development as indicator for environmental change around Karakorum, Upper Orkhon Valley (Central Mongolia), CATENA, 87, 31–44, https://doi.org/10.1016/j.catena.2011.05.005, 2011.

Leyton, L.: The relationship between the growth and mineral composition of the foliage of Japanese larch (Larix leptolepis,
655   Murr.), Plant and Soil, 7, 167–177, https://doi.org/10.1007/BF01343725, 1956.

Liang, M., Sugimoto, A., Tei, S., Bragin, I. V., Takano, S., Morozumi, T., Shingubara, R., Maximov, T. C., Kiyashko, S. I., Velivetskaya, T. A., and Ignatiev, A. V.: Importance of soil moisture and N availability to larch growth and distribution in the Arctic taiga-tundra boundary ecosystem, northeastern Siberia, Polar Science, 8, 327–341, https://doi.org/10.1016/j.polar.2014.07.008, 2014.

660   Lkhagvadorj, D., Hauck, M., Dulamsuren, C., and Tsogtbaatar, J.: Twenty Years After Decollectivization: Mobile Livestock Husbandry and Its Ecological Impact in the Mongolian Forest-Steppe, Human Ecology, 41, 725–735, https://doi.org/10.1007/s10745-013-9599-3, 2013.

Mataix-Solera, J. and Doerr, S. H.: Hydrophobicity and aggregate stability in calcareous topsoils from fire-affected pine forests in southeastern Spain, Geoderma, 118, 77–88, https://doi.org/10.1016/S0016-7061(03)00185-X, 2004.

665 Maximovich, S. V.: Geography and Ecology of Cryogenic Soils of Mongolia, in: Cryosols: Permafrost-Affected Soils, edited by: Kimble, J. M., Springer, Berlin, Heidelberg, 253–274, https://doi.org/10.1007/978-3-662-06429-0_13, 2004.

Nandintsetseg, B. and Shinoda, M.: Seasonal change of soil moisture in Mongolia: its climatology and modelling, International Journal of Climatology, 31, 1143–1152, https://doi.org/10.1002/joc.2134, 2011.

Opp, C. and Hilbig, W.: Regular distribution patterns of soils and plant communities in northern Central Asia with special
670 consideration of the Uvs-Nuur-Basin (in German), Petermanns Geographische Mitteilungen, 147, 16–23, 2003.

Pâques, L. E.: Relationship between foliar nutrient concentrations and growth of hybrid larch (Larix × eurolepsis Henry), Forest Ecology and Management, 63, 153–167, https://doi.org/10.1016/0378-1127(94)90108-2, 1994.

Park, Y. D., Lee, D. K., Stanturf, J. A., Woo, S. Y., and Zoyo, D.: Ecological Indicators of Forest Degradation after Forest Fire and Clear-cutting in the Siberian Larch (Larix sibirica) Stand of Mongolia, Journal of Korean Forest Society, 98,
675 609–617, 2009.

Phu, T. D.: Nutrient requirements of planted European larch in Quebec, Plant and Soil, 42, 109–117, https://doi.org/10.1007/BF02186977, 1975.

R Core Team: R: A language and environment for statistical computing, R Foundation for Statistical, Vienna, 2014.

Sankey, T. T., Montagne, C., Graumlich, L., Lawrence, R., and Nielsen, J.: Lower forest–grassland ecotones and 20th
680 Century livestock herbivory effects in northern Mongolia, Forest Ecology and Management, 233, 36–44, https://doi.org/10.1016/j.foreco.2006.05.070, 2006.

Schlütz, F., Dulamsuren, C., Wieckowska, M., Mühlenberg, M., and Hauck, M.: Late Holocene vegetation history suggests natural origin of steppes in the northern Mongolian mountain taiga, Palaeogeography, Palaeoclimatology, Palaeoecology, 261, 203–217, https://doi.org/10.1016/j.palaeo.2007.12.012, 2008.

685 Schulze, E.-D., Schulze, W., Koch, H., Arneth, A., Bauer, G., Kelliher, F. M., Hollinger, D. Y., Vygodskaya, N. N., Kusnetsova, W. A., Sogatchev, A., Ziegler, W., Kobak, K. I., and Issajev, A.: Aboveground biomass and nitrogen nutrition in a chronosequence of pristine Dahurian Larix stands in eastern Siberia, Canadian Journal of Plant Science, 25, 943–960, https://doi.org/10.1139/x95-103, 1995.

Sharkhuu, N. and Sharkhuu, A.: Effects of Climate Warming and Vegetation Cover on Permafrost of Mongolia, in: Eurasian
690 Steppes. Ecological Problems and Livelihoods in a Changing World, edited by: Werger, M. J. and van Staalduinen, M. A., Springer Netherlands, Dordrecht, 445–472, https://doi.org/10.1007/978-94-007-3886-7_17, 2012.

Sommer, M.: Die Lärchenwälder der Gebirgs-Waldsteppe im Nordwesten der Mongolei (in German): Ökologische Bestandsaufnahmen und Synthese, Dissertation, 2000.

Stüber, V.: Untersuchungen zum standortbezogenen Jugendwachstum der europäischen Lärche (Larix europaea, Dc; Larix
695 decidua, L.) (in German), Zugl.: Göttingen, Univ., Diss., 1998, Cuvillier, Göttingen, 147 pp., 1998.

Sugimoto, A., Yanagisawa, N., Naito, D., Fujita, N., and Maximov, T. C.: Importance of permafrost as a source of water for plants in east Siberian taiga, Ecological Research, 17, 493–593, 2002.

Sympilova, D. P. and Gyninova, A. B.: Soils of the subtaiga landscapes on the northern spurs of the Tsagan-Daban Ridge in the Selenga Mountains, Eurasian Soil Science, 45, 231–236, https://doi.org/10.1134/S1064229312030118, 2012.

700   Timoshok, E. N. and Skorokhodov, S. N.: Ecology of Siberian Stone Pine (Pinus sibirica Du Tour) and Siberian Larch (Larix sibirica Ledeb.) in the Altai Mountain Glacial Basins, Russian Journal of Ecology, 45, 194–200, https://doi.org/10.1134/S1067413614030138, 2014.

Tsogtbaatar, J.: Deforestation and Reforestation of Degraded Forestland in Mongolia, in: The Mongolian Ecosystem Network: Environmental Issues Under Climate and Social Changes, edited by: Yamamura, N., Fujita, N., and Maekawa,

705   A., Springer Japan; Imprint; Springer, Tokyo, 83–98, 2013.

USDA: Soil Survey Field and Laboratory Methods Manual: oil Survey Investigations Report No. 51, Version 2.0. R., 2014.

Viers, J., Prokushkin, A. S., Pokrovsky, O. S., Auda, Y., Kirdyanov, A. V., Beaulieu, E., Zouiten, C., Oliva, P., and Dupré, B.: Seasonal and spatial variability of elemental concentrations in boreal forest larch foliage of Central Siberia on continuous permafrost, Biogeochemistry, 113, 435–449, https://doi.org/10.1007/s10533-012-9770-8, 2013.

710   Wang, H.-M., Wang, W.-J., Chen, H., Zhang, Z., Mao, Z., and Zu, Y.-G.: Temporal changes of soil physic-chemical properties at different soil depths during larch afforestation by multivariate analysis of covariance, Ecology and evolution, 4, 1039–1048, https://doi.org/10.1002/ece3.947, 2014.

Watanabe, M., Ryu, K., Kita, K., Takagi, K., and Koike, T.: Effect of nitrogen load on growth and photosynthesis of seedlings of the hybrid larch F1 (Larix gmelinii var. japonica×L. kaempferi) grown on serpentine soil, Environmental

715   and Experimental Botany, 83, 73–81, https://doi.org/10.1016/j.envexpbot.2012.04.011, 2012.

Wickham, H.: ggplot2: Elegant graphics for data analysis, Use R!, Springer, Cham, 260 pp., 2016.

Zhang, N., Yasunari, T., and Ohta, T.: Dynamics of the larch taiga–permafrost coupled system in Siberia under climate change, Environmental Research Letters, 6, 24003, https://doi.org/10.1088/1748-9326/6/2/024003, 2011.